Nano Research

Open Access

Review Article

Cascade degradation and electrocatalytic upcycling of waste poly(ethylene terephthalate) to valued products

Xin Li[1,§], Zirui Jiang[1,§], Zongkui Kou[2], John Wang[3], and Shiyou Zheng[1]

[1] School of Materials and Chemistry, University of Shanghai for Science and Technology, Shanghai 200093, China
[2] School of Materials Science and Engineering, Wuhan University of Technology, Wuhan 430070, China
[3] Department of Materials Science and Engineering, National University of Singapore, Singapore 117574, Singapore
[§] Xin Li and Zirui Jiang contributed equally to this work.

Cite this article: *Nano Research*, **2025**, *18*, 94907101. https://doi.org/10.26599/NR.2025.94907101

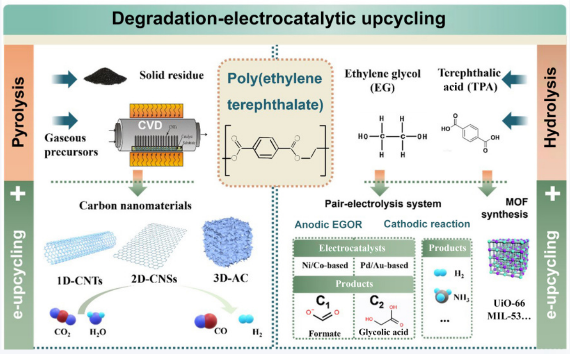

ABSTRACT: The global annual production of poly(ethylene terephthalate) (PET) has reached 82 million tons, yet only a small fraction (less than 20%) is recycled. The ultra-slow degradation rate of PET results in the accumulation of PET waste in the environment, causing serious plastic pollution and posing severe challenges to ecosystems. In response, great efforts have been directed toward developing a cascade degradation and electrocatalytic upcycling strategy, which serves as a "waste-to-wealth" pathway. This strategy involves electro-reforming PET-hydrolyzed intermediates or using PET pyrolyzed products as electrocatalysts to generate high-value products. This review provides an overview of the state-of-the-art strategies for the "degradation-electrocatalytic upcycling (De-eUp)" of PET waste. Initially, an introduction to the strategy is provided, categorizing it into two main frameworks: "pyrolysis-electrocatalytic upcycling" and "hydrolysis-electrocatalytic upcycling". The section on "pyrolysis-electrocatalytic upcycling" delves into the degradation methods for designing derived carbon nanomaterials and their utilization as high-performance electrocatalysts. The "hydrolysis-electrocatalytic upcycling" section discusses recent advancements in electro-reforming of PET hydrolyzed intermediates for the production of C_1 and C_2 products. The review concludes by examining the challenges and future prospects in developing an efficient and economical PET upcycling strategy. It is anticipated that this review will stimulate further progress in plastic waste valorization.

KEYWORDS: poly(ethylene terephthalate) waste, electrocatalytic upcycling, pyrolysis, hydrolysis, ethylene glycol oxidation reaction

1 Introduction

Plastic, a synthetic polymer material derived from monomers through polymerization or polycondensation, has become indispensable in a multitude of daily and industrial applications owing to its cost-efficiency, convenience, processability, and durability [1–3]. Global plastic production reached 348 million tons in 2017, a figure that is growing by ~ 5% annually [4]. The most commonly used plastics, categorized by the type of monomer, include poly(ethylene terephthalate) (PET), polyvinyl chloride (PVC), polypropylene (PP), and others [5]. Among prevalent plastics, PET, which constitutes about 10% of the total plastic usage, predominantly in packaging and textiles, sees an annual production of 82 million tons, with less than 20% being recycled [6–8]. PET is highly resistant to natural, biological, and atmospheric degradation, which takes ~ 300–450 years to decompose naturally [9]. The majority of PET waste enters and accumulates in the environment, causing serious plastic pollution and threatening the aquatic and terrestrial ecosystems [10]. This issue has attracted international attention, highlighting the urgent need for improved recycling and upcycling strategies to manage PET waste effectively [11–14].

Current disposal methods such as landfilling and incineration not only exacerbate environmental issues but also fail to recover economic value from PET waste [15, 16]. Mechanical recycling, the primary method of PET reclamation, often results in inferior quality products, a process termed downcycling [17–19]. Multiple

Received: August 30, 2024; **Revised:** October 27, 2024
Accepted: October 30, 2024

Address correspondence to syzheng@usst.edu.cn

chemical recycling strategies for PET have been proposed and developed, some of which are often costly and energy intensive [20]. To this end, upcycling strategies have been developed as a complementary and more attractive option to explore the inherent value in plastic wastes [17, 21]. Great efforts have been made to develop a cascade degradation and electrocatalytic upcycling strategy. This involves using PET pyrolyzed products as electrocatalysts or electro-reforming PET-hydrolyzed intermediates to generate high-value products.

Recent studies have focused on transforming PET waste into electrode materials for electrocatalysis through processes such as pyrolysis and chemical vapor deposition (CVD) [15]. These processes are designed to synthesize structured carbon nanomaterials that serve as effective electrocatalysts [22, 23]. Specifically, when PET waste is processed under high temperatures in an inert atmosphere, it yields carbon-rich solid residues. Simultaneously, the resultant gaseous hydrocarbons can act as precursors in the CVD process to produce additional carbon-based materials [24–26]. For instance, PET waste-derived one-dimensional (1D) carbon nanotubes (CNTs) [27], two-dimensional (2D) carbon nanosheets (CNSs) [28], and three-dimensional (3D) activated carbon (AC) [29] have been employed in various electrocatalytic applications including hydrogen evolution reaction (HER), oxygen reduction reaction (ORR), carbon dioxide reduction reaction (CO_2RR), etc. Such innovations mark a significant step forward in the upcycling of PET waste, endowing degradation products with valuable electrocatalytic properties.

Electro-reforming, another promising method for PET upcycling, particularly focuses on the ethylene glycol oxidation reactions (EGOR), a component of depolymerized PET [30–33]. Utilizing the PET waste hydrolysate as an electrolyte, electrocatalytic EGOR facilitates the production of high-value chemicals such as C_1 (e.g., formate) and C_2-based hydrocarbons (e.g., glycollic acid) [34, 35]. Consequently, the electrochemical oxidation of PET hydrolysate into products that are both valuable and easy to isolate can be achieved. In addition, assembling an electrolyzer by coupling electrocatalytic EGOR with reduction reaction processes offers an economically viable route for the sustainable upgrading of PET waste and the production of value-added chemicals, which has attracted immense attention in recent years [36, 37]. From the foregoing, advancements have been made in the field of plastic waste upcycling, particularly with the cascade degradation and electrocatalytic upcycling strategy [38–40]. This "waste-to-wealth" pathway, which integrates electrocatalysis powered by renewable electricity and operates under ambient conditions, holds significant potential to make the upcycling process economically viable and profitable [41–43].

In this strategy, electrocatalysis can serve not only as a conversion method for PET waste upcycling but also as an application for PET waste-derived products. Although several comprehensive reviews have summarized electrocatalytic methods and the production of value-added products through PET waste recycling/upcycling [44–47], a systematic and in-depth discussion integrating electrocatalysis as both a conversion strategy and an application in PET upcycling has not yet been presented. This review addresses this gap by exploring the "degradation-electrocatalytic upcycling (De-eUp)" of PET waste and provides a holistic view of the entire electrocatalytic PET upcycling process. When electrocatalysis is used as a conversion strategy for PET waste upcycling, it is referred to as "hydrolysis-electrocatalytic upcycling (h-eUp)", with the selection of electrocatalysts closely related to the transformation products. When PET waste conversion products are used for electrocatalysis, it is termed "pyrolysis-electrocatalytic upcycling (P-eUp)", and the relationship between the conversion process, product structures, and catalytic properties is thoroughly elaborated. Highlighting the dual role of electrocatalysis can stimulate further research and development in this field. Researchers may explore new combinations and applications, leading to breakthroughs in both scientific understanding and practical implementation of PET waste upcycling.

This review introduces the De-eUp strategy and elaborates on its classification into P-eUp and h-eUp at the beginning (Fig. 1).

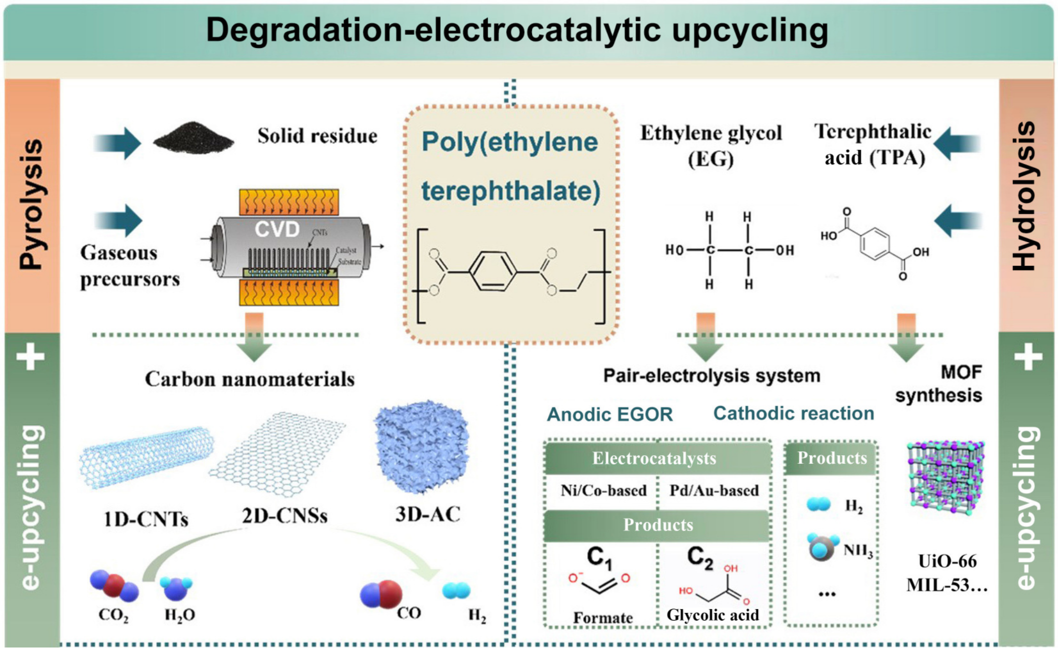

Figure 1 Schematic to introduce the "degradation-electrocatalytic upcycling" strategy for the transformation of waste PET into valued products, including "pyrolysis-electrocatalytic upcycling" and "hydrolysis-electrocatalytic upcycling".

Following this, we systematically review the existing literatures regarding both categories, discussing the advancement and findings to date. For the P-eUp strategy, this review discusses the transformation of PET waste into value-added carbon materials for electrocatalysis, focusing on degradation pathways and the structure–performance relationship of the resultant carbon nanomaterials. For the h-eUp strategy, recent advances in electro-reforming of PET hydrolyzed intermediates towards the production of C_1 and C_2-based hydrocarbons are elaborated upon. Finally, the review concludes with a summary and future perspectives aimed at optimizing PET recycling and upcycling strategies. It is anticipated that this review will provide a comprehensive insight into the De-eUp technique and inspire further advancements in the valorization of plastic waste.

2 Degradation-electrocatalytic upcycling strategy

PET is produced by the polymerization of ethylene glycol ($HO–CH_2–CH_2–OH$) and terephthalic acid (TPA, $C_6H_4(CO_2H)_2$) with an easter linkage [48, 49]. In light of this, PET is a member of the polyester family, with a chemical formula $(C_{10}H_8O_4)_n$ (where n represents the degree of polymerization). PET materials have become an integral part of our daily lives and industries, with their functions and product aspects becoming increasingly important. For example, its high clarity, strength, and barrier properties make it an ideal material for packaging applications such as beverage bottles, food containers, and films for wrapping products [50]. Additionally, PET fibers, also known as polyester fibers, are known for their durability, wrinkle resistance, and easy-care properties, and are extensively used in the textile industry.

However, the non-degradability feature of PET, while advantageous for plastic use, presents severe pollution-related challenges globally [51]. Mechanical recycling is the primary method for PET reclamation, but it is a traditional downcycling approach and the properties of the reclaimed materials often deteriorate relative to raw PET. Therefore, there is an urgent need to develop more effective recycling and upcycling strategies for PET waste treatment [52]. Great efforts have been made to develop a cascade degradation and electrocatalytic upcycling strategy. Products generated from various chemical degradation methods, including pyrolysis and hydrolysis, can be upcycled into new materials, contributing to the circular economy. Further details are provided below.

2.1 Pyrolysis-electrocatalytic upcycling

PET pyrolysis involves chain scission, depolymerization, and deoxygenation at elevated temperatures in the absence of oxygen. This process degrades long-chain polymers into smaller, less complex molecules comprising gaseous, liquid, and solid products [52, 53]. Specifically, the gaseous products include hydrocarbons (e.g., methane, ethylene, propylene), volatile organic compounds, and other low-molecular-weight gases. These gases can be captured and utilized as fuel or further processed for other applications. Additionally, the pyrolysis process yields liquid fractions, such as various hydrocarbon liquids like terephthalic acid, dimethyl terephthalate, and other aromatic compounds. The solid residue remaining in the pyrolysis process is called pyrolytic char or carbon black. The exact composition and distribution of pyrolysis products may vary depending on the specific process conditions and the initial properties of the PET [54]. The complexity of the pyrolysis process complicates the understanding of the reaction mechanisms.

PET contains 62.5% carbon and additional oxygen heteroatoms based on its molecular structure, which is promising for producing valuable carbon-based materials [55]. This conversion not only broadens their applications in electrocatalysis but also contributes to carbon sequestration. In particular, both anoxic pyrolysis carbonization and catalytic carbonization can be used to produce carbon nanomaterials.

Anoxic pyrolysis carbonization, a specific type of pyrolysis aimed at maximizing the carbon content in the residual solid material, effectively produces carbon nanomaterials [56]. According to the International Union of Pure and Applied Chemistry (IUPAC), the definition of carbonization is “a process by which solid residues with increasing content of the element carbon are formed from organic material usually by pyrolysis in an inert atmosphere [57]”. This process, requiring substantial heat and a slow heating rate under an inert atmosphere, gradually and sequentially converts PET waste into valued carbon materials. Pretreatment, focusing on size reduction, is necessary to modify the physicochemical properties of plastics. Ball milling is an effective and environmentally friendly method for reducing plastic particle sizes and ensuring uniform distribution of activators, which typically enhances porous structures and large specific surface area (SSA) [58]. Also, the carbonization temperature significantly affects the product’s physicochemical properties. Generally, higher temperatures (above 700 °C) improve pyrolysis, porosity, and conductivity while reducing oxygen-containing functional groups, making the resulting materials suitable for electrochemical applications. Besides, post-activation using compounds like KOH and chemical modification (e.g., acidic oxidation or doping), are effective strategies to tailor the properties of carbon materialss [59].

Catalytic carbonization, illustrated in Fig. 2, typically involves a dissociation–diffusion–precipitation process facilitated by nanocatalysts. Pyrolysis of PET produces small molecular hydrocarbons that dissociate, with the resulting carbon dissolving into nanoparticles (NPs) and precipitating if supersaturated [60]. The hydrocarbons undergo further decomposition in the presence of transition-metal nano-catalysts [61]. Catalysts facilitate both the initial decomposition and subsequent formation of carbon products. The selection of nano-catalyst is vital for optimizing carbon material production. Numerous catalysts, including those based on Ni and Fe, have been developed for this purpose.

Carbon-based nanomaterials are known for their excellent conductivity and adjustable physicochemical properties, making them candidates for electrocatalysts [62]. The carbon materials obtained from the pyrolysis of PET waste precursors exhibit several advantages when used as electrocatalyst:

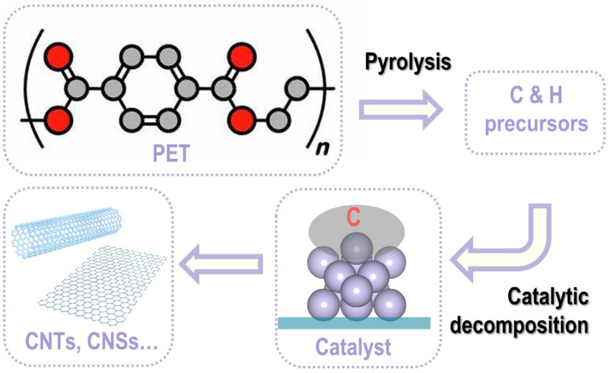

Figure 2 Schematic depiction of pyrolysis and catalytic decomposition of PET for carbon materials with catalyst.

(1) Sustainability and environmental friendliness. Pyrolyzing PET waste to produce carbon materials not only reduces environmental pollution but also achieves effective resource recycling. This aligns with sustainable development principles and contributes to the establishment of a circular economy model.

(2) Structural diversity and tunable properties. Carbon materials derived from PET waste pyrolysis possess rich pore structures, beneficial for mass transport in electrocatalytic reactions. In addition, pyrolysis is highly adaptable, with process parameters such as pressure, temperature, and heating rates being adjustable. This adaptability allows for the derivation of various carbon-based electrodes, including 1D carbon nanotubes, 2D carbon nanosheets, and 3D activated carbon, whose physicochemical properties and electrocatalytic performances are significantly influenced by the synthesis process. Furthermore, carbon materials derived from PET can efficiently incorporate heteroatoms or induce defects within the carbon structure, which can increase the surface active sites and alter electronic density relative to pure carbon, thereby enhancing their electrocatalytic activity.

(3) Cost efficiency. PET waste is typically low-cost or even free, significantly reducing costs compared to other precursors requiring expensive chemicals or high-purity raw materials. Utilizing waste reduces production costs, thereby enhancing economic benefits. Improving the economic viability of plastic pyrolysis and carbon materials production can lead to considerable profits.

Thanks to the advantages as above, the carbon materials obtained from the pyrolysis of PET waste precursors have been employed to electro-catalyze the reactions involving the HER, the ORR, and the CO_2RR, which are significant chemical conversion processes for the production of clean and sustainable energy [63, 64].

In this regard, the concept of "pyrolysis-electrocatalytic upcycling" of PET waste into valuable catalyst shows significant promise in the development of sustainable and eco-friendly technologies [56].

2.2 Hydrolysis-electrocatalytic upcycling

Hydrolysis of PET involves breaking down the polymer into its monomer constituents through a chemical reaction with water [65]. Alkaline hydrolysis can depolymerize PET into TPA and EG monomers by digestion in alkaline solutions (KOH/NaOH) by breaking the ester linkages within the PET polymer chains [66]. This process is commonly used in PET recycling, where post-consumer PET products are treated to recover the original monomers for subsequent polymerization, contributing to the circular economy of PET [38, 67]. TPA can be precipitated and regenerated by adding an acidifier to the PET electrolyte, followed by filtration. Regenerated TPA can be used in PET regeneration, the pharmaceutical industry, metal organic-framework synthesis, etc. For instance, terephthalic acid synthesized from the depolymerization of waste PET via hydrolysis, is also known as 1,4-benzenedicarboxylic acid (BDC). And BDC as an organic linker, can be utilized to synthesize BDC-based metal organic frameworks (MOFs) by reacting with a metal source. With the effective use of waste PET as a BDC linker source, a series of MOF-based materials [68, 69] have been successfully synthesized. In particular, the obtained electrode coupling MOF materials with conductive carbon (i.e., Ni-MOF@CNT) has demonstrated its capability in electro-catalyzing urea oxidation reaction, exhibiting a low onset potential, fast kinetics, and great conductivity [70]. Compared to pyrolysis, hydrolysis does not produce greenhouse gas emissions. However, effective hydrolysis necessitates pre-treatments to remove PET waste impurities and post-treatments to separate small molecule products, indicating potential for process optimization [11].

On the other hand, separating EG is more laborious due to its high boiling point of 197.6 °C and high-water solubility. Therefore, the electrochemical oxidation of EG into value-added and easily isolable products is of great significance. One advantage of this technique is the room temperature operating condition, which is less energy-intensive than conventional heating. Additionally, the *in situ* electrochemical generation of basic conditions in a protic medium eliminates the need for the storage of highly caustic or corrosive solutions, making the system more cost-effective.

Electrocatalytic reactions involve the breaking and formation of chemical bonds and include continuous multistep electron transfer processes. Initially, EG is adsorbed on the catalyst surface. The C–C and C–H bonds of EG are broken to generate intermediates such as glycolaldehyde ($C_2H_4O_2$) or formaldehyde (CH_2O), ultimately forming formate (CHO^{2-}), oxalate ($C_2OO_4^{2-}$), or CO_2, as elaborated in Fig. 3 [11]. EG ($HOCH_2CH_2OH$) contains two hydroxyl functional groups, so the electro-oxidation of EG will produce various C_1 (e.g., formic acid and its derivatives through complete C–C bond cleavage) and C_2 products (e.g., glycolic acid (GA) with C–C bond retained), depending on the degree of oxidation. Formate is used in pharmaceutical, electrolytic metallurgy, leather, and fuel cell applications [71, 72]. GA (approximately $3.1/kg) is essential for producing polyglycolic acid (PGA), a biodegradable polymer with strong market demand [73]. The selection of catalyst, applied potential, and electrolyte environments can exert influences over catalytic mechanism, reaction pathways, and C–C bond cleavage, thereby resulting in the formation of diverse products [74]. Selective electrooxidation of EG to specific products is a worthwhile area of exploration.

For C_2 products, catalyst development strategies have focused on inhibiting C–C bond scission. Noble metal catalysts (e.g., Au, Pt,

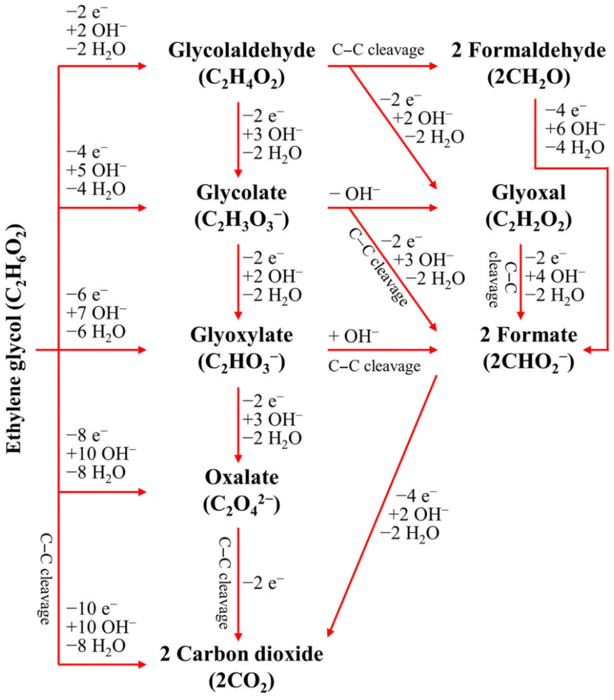

Figure 3 Representative EGOR pathways under alkaline conditions. Reproduced with permission from Ref. [11], © The Royal Society of Chemistry 2023.

Pd) exhibit high selectivity for C–C bond-retained products during alcohol electrooxidation at moderate potentials. In a standard reaction, reactive oxygen species, typically as adsorbed hydroxyl (OH*), are formed through the electrooxidation of H_2O or OH^- on noble metal surfaces at low potentials. These OH* species oxidize alcohols at moderate potentials (< 1.0 V vs. reversible hydrogen electrode (RHE)) to produce C–C bond-retained products like aldehydes, ketones, and carboxylic acids. For example, during the selective oxidation of EG to glycolic acid (Fig. 4(a)), the hydroxymethyl (–CH_2OH) groups in EG undergo continuous dehydrogenation, forming 2-hydroxyacetyl intermediates (*OC-CH_2OH). This is followed by C=O bond activation and –OH coupling, ultimately leading to the formation of GA product [75]. A challenge arises as the potential increases, increasing the likelihood of C–C bond breaking. This creates a balance: higher anode potential results in higher current density and productivity but lower selectivity and Faradaic efficiency (FE) for the C_2 product, while lower current density yields higher selectivity and FE.

In contrast, the primary cleavage of the C–C bonds in PET-derived EG occurs at the anode, requiring a higher anode potential. Unlike noble metal-based electrocatalysts, non-noble metal-based electrocatalysts can produce formate rather than CO_2 through complete oxidation, due to C–C bond scission. Controlled oxidation of EG to produce formate can be achieved using transition metal-based catalysts (e.g., Ni-based catalysts) at higher potentials, indicating that the C–C cleavage pathway dominates (Fig. 4(b)). A higher anode potential enhances depolymerization efficiency but increases energy consumption. Moreover, the two identical hydroxymethyl groups in ethylene glycol, with the chemical formula $(CH_2OH)_2$, pose a challenge to selectivity. A higher current density reduces both selectivity and FE. Therefore, the development of efficient electrocatalysts with well-designed compositions and structures is crucial.

Through the electrocatalytic upcycling, it will be able to depolymerize waste plastics and convert monomers into “hydrogen” energy and functional monomers, making up for the hydrolysis cost. Recent years have seen significant advances in the development of electrocatalysts for the EGOR. However, this research is still in its early stages, as other parameters can be investigated to enhance product yields or increase PET conversion. These variables include tuning the applied potential to change or increase product selectivity, mild heating to raise conversions, testing other solvents, or screening different electrocatalysts to enhance current densities or lower overpotentials. As above, the prospects of “degradation-electrocatalytic upcycling” strategy for the transformation of waste PET into valued products are very promising and are valued by the scientific frontier [55].

3 Pyrolysis-electrocatalytic upcycling strategy

PET is rich in carbon elements, making it one of the most promising sources for preparing high-value carbon materials [76]. In this regard, transforming PET waste into carbon-based electrode materials for electrocatalysis provides an attractive option to upcycle and unlock the hidden value of PET waste [55]. This section is dedicated to summarizing the synthesis of PET derived carbon-based electrocatalysts and discussing their applications for electrocatalysis.

3.1 Conversion of PET waste to carbon materials

Pyrolysis is a thermal degradation process at elevated temperatures in the absence of oxygen. The remaining solid residue from the pyrolysis process can serve as efficient carbon-based electrocatalysts [77]. Also, the main pyrolysis products contain non-condensable gas, which can be employed as gaseous precursors for the CVD process to fabricate carbon nanomaterials.

For instance, AC has been successfully produced by carbonizing PET bottle pieces with KOH activation [29]. This activation process using KOH aims to regulate the structure of products and has been adopted to obtain AC with a high specific surface area and/or a well-defined porous nanostructrure [78]. Another approach for morphology regulation involves the template-assisted carbonization

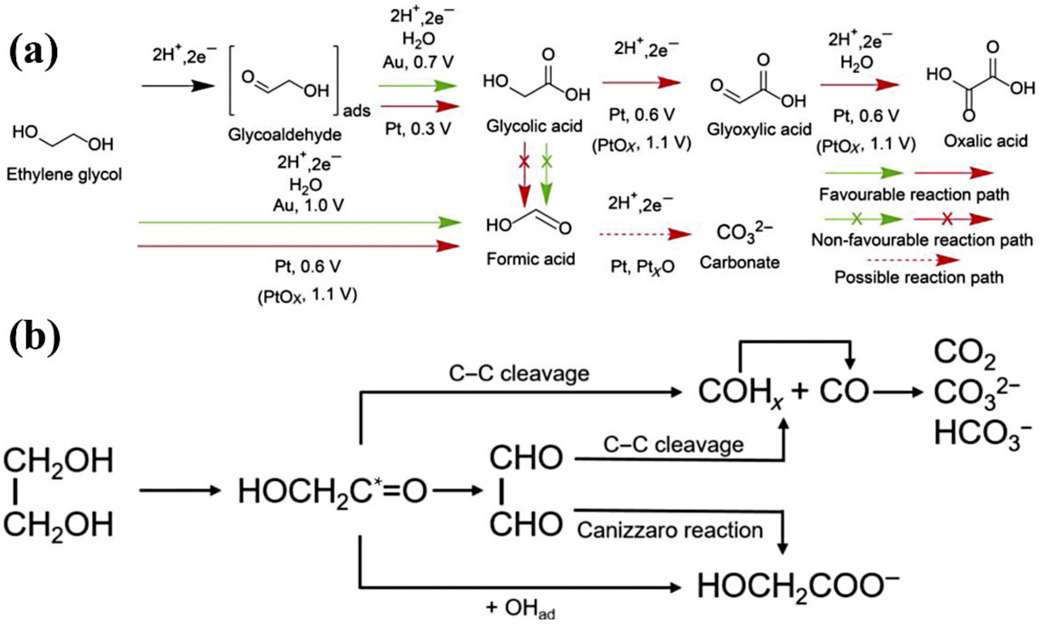

Figure 4 The reaction pathways analysis for electrocatalytic EGOR. (a) The proposed pathways for electrocatalytic EGOR on Au/C and Pt/C in alkaline media, the starting potentials for observed reaction paths are marked. (b) Reaction pathways suggested for electrocatalytic EGOR on Pd and Bi/Pd CNCs in alkaline media. Reproduced with permission Ref. [74], © Elsevier B.V. 2021.

strategy, where waste PET is mixed with a template material to create well-designed carbon-based nanomaterials [79]. For example, Zhang et al. [76] selected MgO as a template considering its cost-effective, morphology-tunable, and removable characteristics. They evenly mixed waste plastics (such as PET masks) with MgO in a mortar at room temperature. After carbonization, the MgO template can be easily removed by pickling, resulting in the production of porous carbon. In addition to structure control, the involvement of defects is also an effective strategy to improve the qualities and properties of the as-obtained carbon materials. During the synthesis process, urea or other nitrogen-containing precursors can serve as a nitrogen source and be added to realize nitrogen doping [76]. Nitrogen doping can also be achieved by a nitric acid-assisted hydrothermal approach to obtain N-doped carbon nanotubes [80]. Interestingly, Selvakumar et al. [29] adopted a nitrogen doping-dedoping strategy in order to create defects. They synthesized high nitrogen content activated carbon through a hydrothermal method using urea as a nitrogen source and then heated the obtained powder to 800 °C in an Ar atmosphere to create defective sites.

It is worth noting that CVD after pyrolysis has also shown the potential to convert PET waste into carbon nanomaterials [81]. As known to us, the main pyrolysis products contain non-condensable gas, which can be employed as gaseous precursors for the following CVD process to fabricate carbon materials. During the CVD process, gaseous hydrocarbon precursors react on or in the vicinity of a normally heated substrate surface at a certain temperature, decompose to form carbon radicals and then generate carbon materials [25, 82, 83]. In catalytic CVD, a catalytic material is introduced into the reaction chamber along with the precursor and carrier gases. For example, Lisak et al. [81] employed a CVD approach to successfully develop multiwalled carbon nanotubes (MWCNTs) with the catalysis of a nickel-based catalyst [27], which showed remarkable catalytic activity for ORR. Indeed, the catalyst plays a crucial role in promoting the desired chemical reactions during the deposition process. It has been demonstrated that the physicochemical properties of Cu-based catalysts for catalytic CVD influenced the carbon yield and CO_2RR performance of the products [28].

Recently, Luong et al. [84] developed an alternative approach to transform carbon sources to graphene, which is termed as direct current flash Joule heating (DC-FJH). This strategy relies on electricity to induce flash Joule heating, driving the mixed plastic to high temperatures in a short period and converting them into gram-scale flash graphene (FG) in 1 s. Subsequently, this research group developed an improved technology named alternating current flash Joule heating (AC-FJH) [85]. Unlike DC-FJH, AC-FLH strategy can be sustained for seconds (~ 8 s), allowing for the release of necessary volatiles. It has been revealed that the sequential AC and DC (ACDC) flash process was effective for upcycling plastic waste mixtures to obtain high-quality turbostratic flash graphene (tFG). Although the obtained graphene has not been applied for electrocatalysis as of now, this technology demonstrated its potential for developing PET-derived carbon-based electrocatalysts. Further research and development in this area may unlock the hidden value of plastic waste and contribute to sustainable recycling practices.

3.2 Electrocatalytic upcycling of PET-derived carbon

1D CNTs offer great potential in a wide range of electrochemical applications ascribed to their excellent conductivity, abundant active edge sites, and good mechanical strength. Lisak et al. [81] employed a CVD approach to successfully develop MWCNTs with the catalysis of a nickel-based catalyst. During the CVD process, the non-condensable pyrolysis gases produced by pyrolyzing mixed plastic acted as the precursors. The researchers further investigated the effects of CVD temperature on the properties of PET-derived carbon nanotubes for electrocatalytic ORR. Raman and X-ray photoelectron spectroscopy (XPS) analysis demonstrated that the CNTs synthesized at 500 °C possessed a higher density of edge defects than those synthesized at 800 °C, as a higher CVD temperature led to the annealing and oxidation of edge defects. As expected, CNTs synthesized at 500 °C exhibited superior ORR properties with an onset potential ranging from −0.11 to −0.14 V, thanks to their richer edge defects, which served as active sites for ORR. Subsequently, the same research group [27] adopted a similar pyrolysis and CVD strategy to process flexible plastic packaging waste containing PET. They also considered the catalytic oil upgrading process in this work, which would not be elaborated more as it is beyond the scope of this review. As a result, the obtained MWCNTs gave rise to great catalytic activity for ORR (Figs. 5(a)–5(c)). These studies suggested the successful transformation of PET waste into one-dimensional carbon nanotubes via a pyrolysis-CVD strategy and demonstrated their great potential as an alternative ORR electrocatalyst with high performance.

2D CNSs enable a uniform dispersion of metal electrocatalysts and promote contact with the electrolytes when serving as catalyst supports [86]. Additionally, CNSs ensure the great stability of the electrocatalyst by encapsulating metal particles in graphitic layers or forming covalent bonds. In addition, the large surface area of 2D nanomaterials allows for enhanced chemical reactivity and functionalization, expanding their potential applications in catalysis, sensing, and biomedicine [87].

To this end, the PET-derived 2D CNS for electrocatalysis has aroused great interest among researchers. Lisak et al. [28] indicated that considerable amounts of metal-impurities would be introduced into the produced carbon materials during the catalytic CVD process because of the metallic catalyst involvement. Taking advantage of this, they utilized Cu-loaded CaO (Cu/CaO) as a catalytic CVD catalyst because not only can Cu effectively catalyze CVD growth of carbon nanomaterials, but also Cu-based materials have been extensively studied as a promising CO_2RR electrocatalyst (Figs. 5(d) and 5(e)). As anticipated, the PET waste could be transformed into CNS encapsulating Cu electrocatalyst via a catalytic CVD process. It is worth noting that the physicochemical properties of Cu-based catalysts for catalytic CVD would influence the carbon yield and CO_2RR performance of the products. To prove this, different Cu/CaO catalysts with varying nanoparticle sizes and porosity degrees were synthesized through various impregnated approaches with or without additives (Fig. 5(f)). Figures 5(g) and 5(h) demonstrated that urea-assisted preparation of Cu/CaO gave rise to the Cu/CNS composites with uniformly dispersed Cu nanoparticles, optimized Cu-particle size, well-defined porosity, and the highest carbon yield. As shown in Fig. 5(i), the synthesized CNS-supported Cu electrocatalyst showed great CO_2RR properties with the best CO selectivity (FE = 82.1% at −0.76 V vs. RHE). Additionally, Zhang et al. [76] utilized a facile carbonization approach, successfully converting plastic waste (such as PET) into layered porous nitrogen-doped carbon sheets (LPNCS). The as-prepared LPNCS with a high degree of graphitization and well-defined hierarchical porous structure could

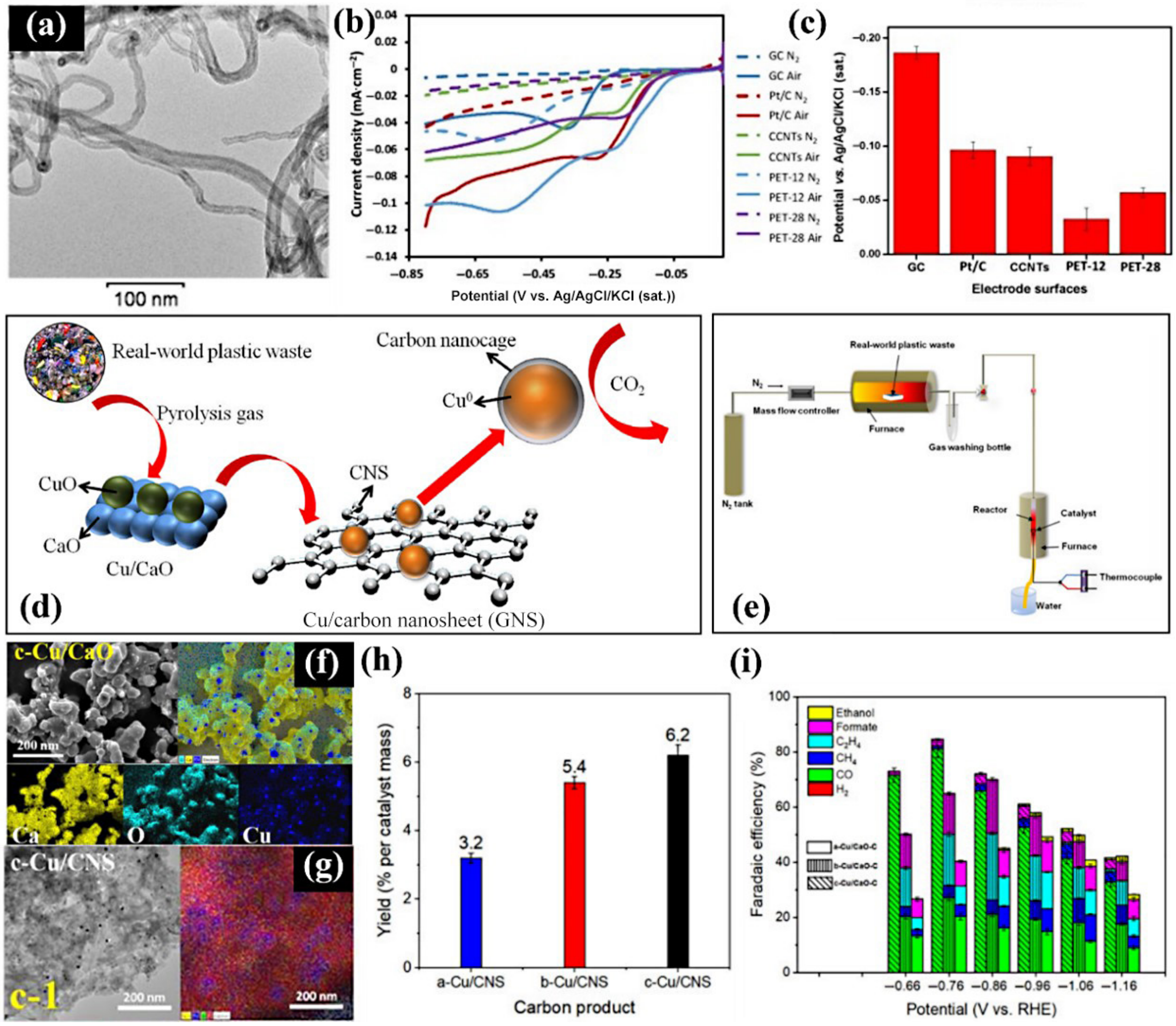

Figure 5 (a) Transmission electron microscopy (TEM) images of MWCNTs from PET-12. (b) LSVs of ORR and (c) onset potential values. All measurements were triplicated. Reproduced with permission Ref. [27], © Elsevier B.V. 2019. (d) and (e) CCVD synthesis of Cu/CNS from real-world plastic waste. (f) Field emission scanning electron microscopy (FESEM)/energy dispersive spectroscopy (EDS) images of Cu/CaO catalysts. (g) TEM images of c-Cu/CNS with EDS elemental mapping. (h) Yield of synthesized carbon over different Cu/CaO and (i) FEs for CO_2RR products obtained on a-, b-, and c-Cu/CNS at various potential range. Reproduced with permission Ref. [28], © Elsevier Ltd. 2021.

serve as an ideal support for Ru loading, which promoted Ru dispersion and reduced the mass transfer resistance during the hydrogen evolution reaction. The prepared Ru/LPNCS showed superior HER properties compared to those reported for Ru-based electrocatalysts and commercial Pt/C electrocatalysts, with the overpotential being as low as 15 mV at 10 mA·cm^{-2}.

3D AC features a highly porous structure with a large specific surface area and abundant pore capacity, making it an ideal catalyst support that facilitates active sites enrichment, promotes reaction kinetics, and enhances mechanical stability [88]. Researchers have reported the synthesis of 3D flower-like AC from PET bottles [29]. In this work, the prepared AC underwent nitrogen-doping and subsequent dedoping to induce defects. This approach resulted in optimized AC with a higher amount of microporosity, leading to an improved specific surface area from 899 to 980 m^2·g^{-1}. Subsequently, the plastic PET bottle-derived AC (PDAC) was combined with MoS_2 to create the PDAC/MoS_2 composite, which was investigated as a promising HER electrocatalyst. The composite exhibited an overpotential of −192 mV and a Tafel slope value of 82 mV·dec^{-1}.

4 Hydrolysis-electrocatalytic upcycling strategy

In order to advance the goal of a circular economy, hydrolysis as one of the most promising chemical recycling strategies can depolymerize PET waste to attractive monomers or oligomers, which has attracted much attention. To be specific, alkaline hydrolysis can depolymerize PET into TPA and EG monomers by digestion in alkaline solutions (KOH/NaOH). Upcycling has been proposed to solve the low profitability of known recycling methods and create additional practical and economic benefits. Electrocatalytic upcycling of PET has garnered increasing attention as an environmentally friendly, energy-efficient, and sustainable strategy [23, 37].

4.1 Electrocatalytic upcycling of ethylene glycol

As is known to us, separating ethylene glycol is laborious due to its high boiling point of 197.6 °C and high-water solubility. Therefore, the electrochemical oxidation of EG into value-added and easily isolable products is of great significance.

Interestingly, $HOCH_2CH_2OH$ contains two hydroxyl functional groups, so the electro-oxidation of EG will produce various C_1 and C_2 products such as formate and glycolic acid, depending on the degree of oxidation. That is to say, the selection of catalyst and electrolyte environments can exert influences over catalytic mechanism, reaction pathways, and C–C bond cleavage, thereby resulting in the formation of diverse products. Recent years have witnessed great advances in the development of electrocatalysts for EGOR [74], and this section overviewed recent progress of EGOR for the PET waste upcycling.

4.1.1 *Electrocatalytic ethylene glycol oxidation to C_1 products*

In the electro-reforming process, the waste PET hydrolysate containing EG monomers, is able to be selectively oxidized to C_1 products such as formate.

4.1.1.1 Pair-electrolysis system coupling EGOR and HER

Aiming to upcycle PET waste, Duan et al. [89] were the first to report the "electro-reforming strategy (ERS)". This strategy necessitates a pair-electrolysis system coupling EGOR and HER, with the electrolyte being PET waste hydrolysate containing EG monomers (Fig. 6(a)). Duan et al. demonstrated that this proposed ERS strategy would be profitable when ethylene glycol can be efficiently oxidized with high selectivity achieving more than 80% at a high current density of above 100 $mA·cm^{-2}$, according to their techno-economic analysis in Fig. 6(b). To get that requirement, a bifunctional electrocatalyst $CoNi_{0.25}P$ was designed and employed in this pair-electrolysis system. Based on the experimental results and comprehensive analysis (Figs. 6(c) and 6(d)), the $CoNi_{0.25}P$ catalyst was found to transform into oxyhydroxide with low crystallinity during anodic EGOR, while being reconstructed into a

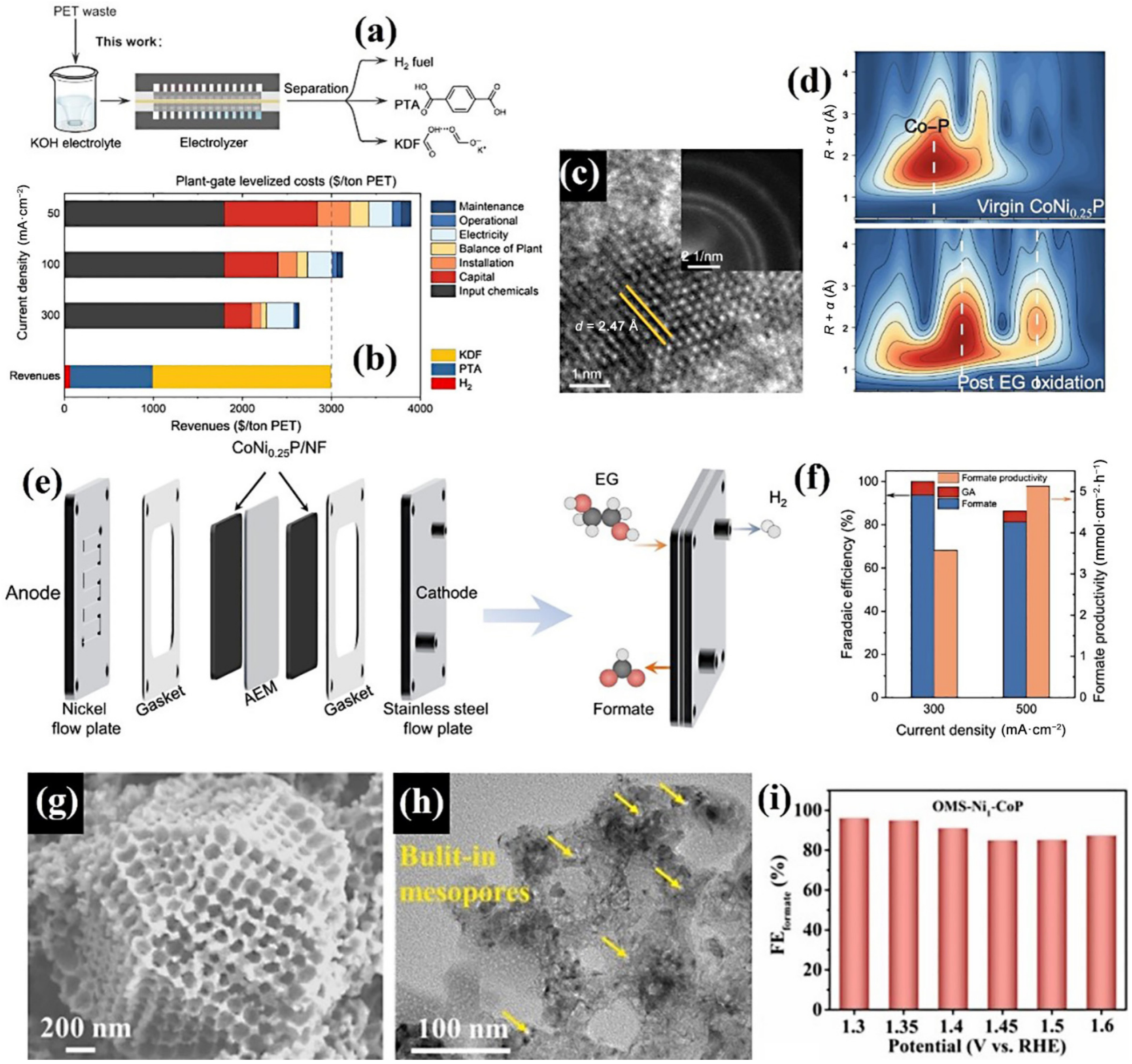

Figure 6 (a) Conceptual design: Electrocatalytic PET upcycling to commodity chemicals and H_2 fuel. (b) Techno-economic analysis (TEA) at different current density. (c) TEM images and corresponding selected area electron diffraction (SAED) patterns of $CoNi_{0.25}P$ after EG oxidation reaction for 1 h. (d) Wavelet transforms for Co K-edge extended X-ray absorption fine structure (EXAFS) spectra for virgin and spent $CoNi_{0.25}P$. Membrane-electrode assembly (MEA) for EG oxidation: (e) The MEA setup for paired HER(−)//EG oxidation(+). (f) Faradaic efficiency and productivity as function of current density for EG oxidation. Reproduced with permission Ref. [89], © Zhou, H. et al. 2021. (g) Representative SEM images of OMS-Ni1-CoP at different magnifications. (h) TEM images of OMS-Ni_1-CoP at different magnifications. (i) The FE of OMS-Ni_1-CoP for formic acid production under different potentials. Reproduced with permission Ref. [90], © Elsevier B.V. 2022.

core–shell structure composed of metal phosphide core and oxyhydroxide shell under cathodic HER. Duan et al. [89] further indicated that the *in situ* evolution of the phosphide into a metal oxyhydroxide analogue with low crystallinity may lead to advantageous performance for EG oxidation. In the assembled membrane electrode reactor as shown in Fig. 6(e), the catalyst exhibited high current density (~ 500 mA·cm^{-2} at 1.8 V) and excellent selectivity to formate (> 80%) (Fig. 6(f)). This work paves the way for a sustainable and profitable path for the upcycling of PET waste and the production of value-added chemicals.

Subsequently, inspired by the remarkable catalytic activity of transition metal phosphides for ethylene glycol oxidation reaction, a wide range of transition metal-based oxides/non-oxides have been developed and revealed to be promising for electro-catalyzing ethylene glycol oxidation to C_1 products (e.g., formate). These include nickle/cobalt-based oxides/hydroxides [91], non-oxides (phosphides, nitrides, sulfides) [90, 92], and others (polymers, etc.). The main product of EG on these electrodes in alkaline media is formate, demonstrating that the C–C cleavage pathway is dominant. For example, a nickel-based hydroxide $Ni(OH)_2$ electrocatalyst has been developed using a simplified acid etching method. As has been revealed by the *in situ* electrochemical Raman spectroscopy, $Ni(OH)_2$ was oxidized and a large amount of NiOOH species was formed. The produced oxyhydroxide species could act as an oxidant facilitating the oxidation reaction, leading to improved catalytic activity for PET hydrolysate oxidation. In an assembled cell, $Ni(OH)_2$/NF achieved a FE of more than 90% and high formate selectivity even at industrial grade current densities [18]. Also, a self-supported amorphous cobalt iron phosphide electrode, CoFe-P, was designed for the HER and the selective electrooxidation of PET hydrolysate to formate. Utilizing the abundant catalytic sites within its amorphous structure, interelement synergy, and extensive exposure to the electrolyte, the PET hydrolysate electrolysis system employing CoFe-P enables the co-production of H_2 and valuable formate at reduced voltage (1.52 V at $j = 20$ mA·cm^{-2}) and energy consumption (84% at $j = 200$ mA·cm^{-2}) compared to water electrolysis [93].

Studies have also found that not only nickel/cobalt-based inorganic catalysts, but also some organic ones can catalyze the electrochemical reforming of PET hydrolysate. The PdNi O-BMs catalyst exhibits superior catalytic activity and stability in the EGOR process, primarily due to the incorporation of Ni and the modification with n-octanoic acid, which fine-tunes the electronic configuration of the Pd material and provides a high number of active sites. As a result, the PdNi O-BMs catalyst, characterized by a frizzy and porous structure, has demonstrated its effectiveness in the electrocatalytic production of formic acid from waste PET plastics [94].

To enhance the properties of catalysts, researchers are making efforts to develop advanced electrocatalysts through rational structural engineering, defect engineering, and interface engineering strategies.

Rational structural engineering. A freestanding Co-Ni_2P electrode with a nanosheet-like morphology was designed and adopted as a bifunctional electrocatalyst. This 2D nanosheet-like structure offered a high specific surface area, excellent electrical conductivity, and abundant active sites. As a result, an electrolyzer assembled by coupling EGOR and HER enabled a high Faradaic efficiency of 85% for formate, and only required 1.43 V to reach 10 mA·cm^{-2} [92]. Furthermore, Zhu et al. [90] developed a Ni-CoP electrocatalyst with an ordered macroporous superstructure featuring abundant built-in mesopores, which can be seen in Figs. 6(g) and 6(h). This distinctive structure inherited from parent MOFs (ZIF-67 single crystals), endows the Ni-CoP electrocatalyst with outstanding activity, and the Faradaic efficiency of formate achieved up to 96% in alkaline electrolyte during EGOR (Fig. 6(i)).

Defect engineering. In addition, the defect engineering strategy has been studied to upgrade the electrocatalytic performance [95]. For instance, the redox behavior of Ni^{2+}/Ni^{3+} could be promoted by introducing Co into Ni_3N/carbon cloth (CC). Accordingly, the EG oxidation could be electro-catalyzed at an ultra-low potential, overcoming the high potential problem of nickel-based catalysts [96]. Similarly, Ni et al. [97] prepared a B,Co-NiS electrocatalyst for effectively transforming real PET waste into formate. The defect engineering strategy through anion(B)-cation(Co) co-doping process enhanced the catalytic properties of nickel sulfide electrocatalyst. The dopant could facilitate the *in situ* evolution of B,Co-NiS electrocatalyst, leading to the formation of a core@shell structure composed of sulfide@oxyhydroxide phase. As a result, the bifunctional B,Co-NiS electrocatalyst could drive real PET waste hydrolysate electrolysis in a membrane electrode assembly (MEA), generating 15.24 mmol formate per hour and achieving H_2 production efficiency over 70 times compared to conventional water electrolysis. Additionally, Chen et al. [98] successfully synthesized cobalt-based spinel oxide $NiCo_2O_4$, with a well-designed architecture of rod-shaped nanofibers (RSFs). To explore the effects of Mn doping into $NiCo_2O_4$ on the catalytic activity for ethylene glycol oxidation, a series of electrocatalysts $Mn_xNi_{1-x}Co_2O_{4-\delta}$ (x = 0, 0.01, 0.1, or 0.5) with different Mn doping ratios were developed. As a result, $Mn_{0.1}Ni_{0.9}Co_2O_{4-\delta}$ RSFs achieved > 95% Faradaic efficiency at 1.42 V with optimized formate production, which was the highest among the $Mn_xNi_{1-x}Co_2O_{4-\delta}$ electrocatalysts.

Interface engineering. Besides, heterostructure engineering has proven effective in optimizing adsorption energies and promoting catalytic activation for both EGOR to formate and HER. For example, a heterostructure consisting of Ni_3N and $Ni_{0.2}Mo_{0.8}N$ has been prepared [99]. In this interface-engineered electrocatalyst, electrons transfer from $Ni_{0.2}Mo_{0.8}N$ to Ni_3N with the accumulation of holes on $Ni_{0.2}Mo_{0.8}N$, facilitating the anodic EG oxidation and enhancing the EGOR performance. Additionally, a heterogeneous interface structure can facilitate the electron transfer and enrich active sites. Wang et al. [35] developed a hetero-structured electrocatalyst composed of Ni_3P nanoparticles and $NiMoO_4$ nanowires, which efficiently catalyzed the PET hydrolysate oxidation to formate with a maximum FE of 92.2%. Likewise, the interfacial engineering of Pd-deposited hierarchical aligned NiTe nanoarrays (Pd-NiTe) for the synergistic coupling of PET upcycling with HER was explored. The strong interfacial electronic interactions between Pd and NiTe enhance the performance of Pd-NiTe/NF in both HER and the oxidation of PET hydrolysate [100]. Besides, the electrochemical deposition of Cu on Ni foam (denoted as NiCu/NF) for the upcycling of EG was also investigated [101]. The incorporation of Cu into Ni foam enhances the formation of Ni^{3+} active species and improves EG oxidation kinetics through enhanced interfacial electron transfer. The presence of Cu facilitates C–C bond cleavage by reducing the ΔG of $*COOHCH_2OH$ to $*CH_2OH + HCOOH$. Consequently, NiCu/NF exhibited markedly improved FE (95.8%) and yield rate (0.70 mmol·cm^{-2}·h^{-1}) for formate production compared to pristine NF.

4.1.1.2 Pair-electrolysis system coupling EGOR and other reduction reactions

Not only can the electrochemical oxidation of ethylene glycol be coupled with the hydrogen evolution reaction in a pair-electrolysis system for upcycling PET waste, but it can also be coupled with other appropriate cathodic reduction reactions. Indeed, the coupling of the electrooxidation of PET hydrolysate with the CO_2RR for CO_2 reduction, with the ORR for H_2O_2 production, and with the nitrate reduction reaction (NO_3RR) for NH_3 production [102] has been developed.

As shown in Fig. 7(a), Ma et al. [103], reported a pair-electrolysis system that coupled EGOR with CO_2RR to achieve the electro-reforming of PET waste through PET hydrolysate oxidation. Specifically, they prepared an interface-engineered electrocatalyst consisting of $NiCo_2O_4$ nanowire and SnO_2 nanosheet electrodes. The $NiCo_2O_4$ nanowires were utilized for the electrocatalytic EG oxidation, while the SnO_2 nanosheets facilitated the electroreduction of CO_2 (Fig. 7(b)). This assembled electrolyzer achieved a high Faradaic efficiency of above 100% (155%) for formic acid production at a cell voltage of 1.9 V, because value-added formic acid could be produced concurrently at both the anode and the cathode (Fig. 7(c)). Recently, a novel electrosynthesis system integrating cathodic ORR-to-H_2O_2 with anodic PET upcycling has been developed. The Ni_1Mn_1-MOF-Se catalyst, enhanced by high-valence Mn and heteroatom Se, exhibits superior EG oxidation performance, requiring overpotentials of 1.362 V for current densities of 400 mA·cm^{-2}, respectively. On the cathodic side, the B/N-onion carbon catalyst achieves an ORR-to- H_2O_2 FE of 97.5% at overpotentials of 0.60 V for current densities of 400 mA·cm^{-2}. The ORR || PET upcycling system operates at low cell voltages of 0.927 V for industrial-scale current densities of 400 mA·cm^{-2}, outperforming existing H_2O_2 electrosynthesis systems [104].

Another example involves coupling PET upcycling with the NO_3RR. Figures 7(d) and 7(e) showed that a nanosheet-like pre-catalyst composed of Co-based MOF encapsulating Ru (CoRu-MOF) was successfully grown on nickel foam (NF). During the reaction, the CoRu-MOF pre-catalyst would be *in situ* reconstructed to Ru-Co(OH)$_2$ under the cathodic NO_3RR, while it would be reconstructed to Ru-CoOOH at the anode for PET hydrolysate oxidation, which can be seen in Fig. 7(f) and 7(g). For anodic EG oxidation, the reconstructed Ru-CoOOH, instead of MOFs, functioned as real active catalysts. This led to the formation of more hydroxylated species as electron-proton conductors,

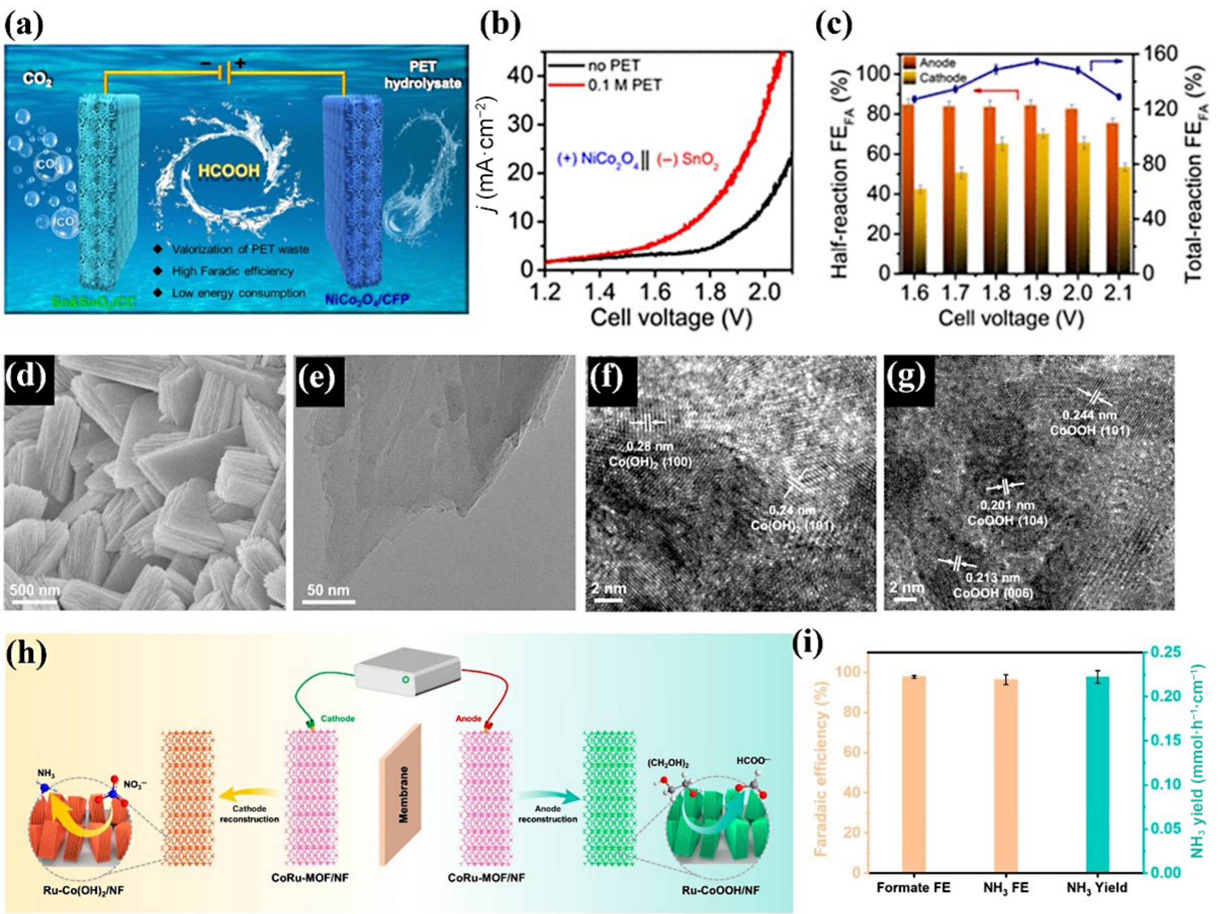

Figure 7 (a) Concurrent electrochemical conversion of anodic PET hydrolysate and cathodic CO_2 to formic acid. Electrochemical performance of the SnO_2||$NiCo_2O_4$ system. (b) LSV curves for the SnO_2||$NiCo_2O_4$ electrolytic cell with and without the existence of 0.1 M PET hydrolysate in the anode cell. (c) Faradaic efficiencies of $NiCo_2O_4$/CFP for PET hydrolysate oxidation and SnO_2/CC for the CO_2RR to produce formic acid at different applied cell voltages. Reproduced with permission Ref. [103], © American Chemical Society 2022. (d) SEM and (e) TEM images of CoRu-MOF/NF. HRTEM image of (f) Ru-Co(OH)$_2$ and (g) Ru-CoOOH. (h) Schematic illustration of the electrocatalytic system for NO_3RR and PET hydrolysate upcycling. (i) CoRu-MOF/NF precatalyst as cathode and anode in (−)NO_3RR//PET hydrolysate oxidation(+) and (−)NO_3RR//OER(+). Formate Faradaic efficiency, NH_3 Faradaic efficiency and yield rates over the CoRu-MOF/NF precatalyst at 2.3 V. Reproduced with permission Ref. [105] © American Chemical Society 2023.

promoting the oxidation reaction and yielding a high Faradaic efficiency of 96.53% for formate production at 1.33 V vs. RHE. Furthermore, an electrolyzer coupled with NO_3RR was assembled, which could produce formate at the anode and yield NH_3 at the cathode (Fig. 7(h)). As shown in Fig. 7(i), a high current density of 50 $mA{\cdot}cm^{-2}$ could be achieved at a low cell voltage of 1.53 V, which was considered energy-saving [105]. These research findings and advances will further expand the prospects of PET waste upcycling through the utilization of the electro-reforming strategy.

4.1.2 *Electrocatalytic ethylene glycol oxidation to C_2 products*

The controlled oxidation of ethylene glycol to produce high-value C_2 products like glycolic acid is also technically and economically feasible. Glycolic acid contains both a carboxyl group and a hydroxyl group, which exibits extraordinary chemical characteristics [73]. Indeed, glycolic acid is a crucial industrial raw material widely used in various industrial applications, such as metal cleaning, textiles, health-care products, adhesives, and so on. Generally, when employing noble metal-based catalysts that show catalytic oxidation capability towards ethylene glycol, e.g., Au-based catalysts and Pd-based catalysts, the oxidation products are dominant by C_2 chemicals at relatively low potential during the ethylene glycol oxidation reaction.

During the selective oxidation of EG to glycolic acid, the hydroxymethyl ($-CH_2OH$) groups in EG undergo continuous dehydrogenation, resulting in the formation of $*OC\text{-}CH_2OH$. This is followed by C=O bond activation and –OH coupling, ultimately leading to the formation of GA product. This cascade electrocatalytic process is critical for the conversion of EG to GA. On the other hand, the two identical hydroxymethyl groups in ethylene glycol with a chemical formula of $(CH_2OH)_2$ pose a challenge to selectivity.

In this regard, it is important to enrich reactive intermediates on catalysts and prevent overoxidation or C–C bond cleavage to increase the catalytic activity and selectivity. And the rational assembly of composite electrocatalysts by interface engineering is significant. Shao et al. [19] developed a catalyst composed of Au decorated $Ni(OH)_2$ (Fig. 8(a)). During the reaction, EG molecules tended to form alkoxide forms, which could be enriched at the interface of this heterostructured catalyst by forming a σ bond with Au and hydrogen bond with $Ni(OH)_2$ (Fig. 8(b)). As displayed in Fig. 8(c), reactive oxygen species OH* generated over the Au surface at low potential enabled to oxidize alcohol dehydrogenation to generate C_2 products GA. Consequently, the $Au/Ni(OH)_2$ catalyst achieved selective electrooxidation of EG-to-GA with a high selectivity of around 91% at high current density (326.2 $mA{\cdot}cm^{-2}$ at

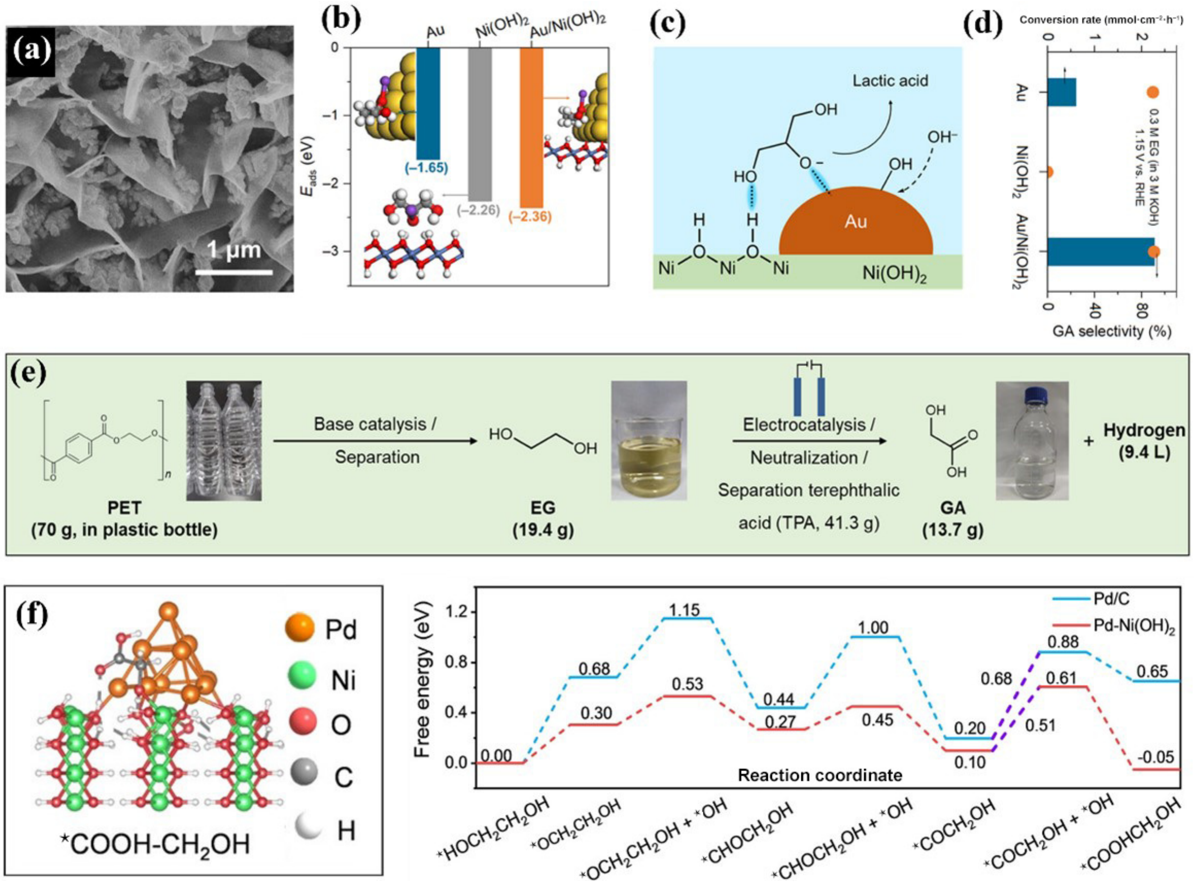

Figure 8 (a) SEM image of the $Au/Ni(OH)_2$ catalyst. (b) Adsorption energies of GLY in the form of alkoxide on Au, $Ni(OH)_2$, and $Au/Ni(OH)_2$, respectively. The optimized geometries of $(HOCH_2)_2CH_2O\text{-}*$ for Au, $Ni(OH)_2$, and $Au/Ni(OH)_2$ are also displayed. The color of each element is yellow for Au, blue for Ni, red for O, white for H, gray for C, and purple for K. (c) Schematic illustration of the adsorption configuration of glycerol alkoxide at the $Au/Ni(OH)_2$ interface. (d) Conversion rate of EG and the corresponding selectivity of GA over different catalysts. (e) Kinetic curves for GLY (top) and EG (down) electrooxidations over $Au/Ni(OH)_2$. (e) Schematic illustrations of the electrocatalytic upgrading process of waste PET bottles. Reproduced with permission Ref. [19], © American Chemical Society 2023. (f) Crystal structure of the $Pd\text{-}Ni(OH)_2$ and Gibbs free energy diagrams for EG-to-GA oxidation on Pd and $Pd\text{-}Ni(OH)_2$ (0 V vs. RHE). The numbers are the Gibbs free energies with units in eV. Reproduced with permission Ref. [106], © Wiley-VCH GmbH 2023.

1.15 V vs. RHE) and moderate potentials, indicating its potential for practical metrics (Fig. 8(d)). Then they upcycled PET bottles using this catalytic system, as shown in Fig. 8(e), producing 13.7 g of GA (81.6% yield) and 9.4 L of H_2. These findings highlight the importance of interface engineering and composite catalysts for the selective electrooxidation of EG to produce high-value C_2 products such as GA. The interactions at the interface not only can enrich the intermediates, but also can modulate the electronic structure of active sites. Taking Pd/Ni$(OH)_2$ and Pt/Ni$(OH)_2$ catalysts for EG-to-GA oxidation as examples, Chen et al. [106] delved into the synergistic effects between constitutes. They found that the interface effects caused a downshift in the d-band center of Pd, leading to a decrease in the adsorption energy of GA and facilitating its desorption, which has been proved by the further calculation results in Fig. 8(f). At the meanwhile, the oxophilicity of Ni increased, promoting the transfer of GA from active Pd sites to inactive Ni sites. Therefore, the over-oxidation of GA or C–C bond cleavage could be avoided. Then an electrolyzer coupling PET hydrolystae oxidation and HER was assembled. The results showed that 100 g of PET raw materials produced 23.2 g GA (yield: 58.5%) at 100 mA·cm^{-2} under a 1.2 V cell voltage, demonstrating its potential in the practical application value. Likewise, the catalyst Pt/Ni$(OH)_2$ composed of Pt nanoparticles and Ni$(OH)_2$ nanosheet could operate at a low potential of 0.69 V vs. RHE to achieve a current density of 100 mA·cm^{-2} for the selective electrochemical reforming of waste PET-derived EG to GA with a high FE (~ 93%) in alkaline conditions. Density functional theory (DFT) calculations further revealed that the electronic interaction between Pt and Ni$(OH)_2$ enhances GA desorption from the Pt surface, preventing overoxidation or C–C bond cleavage of GA. In particular, Ni$(OH)_2$ efficiently generates ·OH species, which remove adsorbed toxic *CO intermediates, thereby improving catalytic stability [107].

Furthermore, alloy-based catalysts also display synergistic effects in the transformation of PET waste into glycolate C_2 products. For example, Pd atoms act as active sites for EGOR. However, the strong interaction between Pd and carbonyl (*CO) intermediates often leads to over-oxidation and poisoning of Pd sites, hindering efficient C_2 product production. Alloying with Ag atoms modulates the electronic structure of Pd, thereby reducing the adsorption energy of glycolate at the Pd site [108]. In this way, the unnecessary excessive oxidation of GA could be prevented. In addition, Ag sites induced the formation of active oxygen species (*OH) thanks to their high affinity with water, promoting the oxidation of toxic carbonyl species and contributed to the stability of the Pd active sites. Chen et al. [108] utilized a strong reducing agent to fabricate a segregation-less PdAg NP alloy, ensuring the exposure of more surface Ag sites. As expected, the PdAg NPs demonstrated high selectivity (> 90%) and excellent durability (> 500 h) during the upcycling of PET waste into glycolate. Interestingly, introducing nonmetallic B atoms to form a Pd-boron (PdB) alloy aerogel also could enhance surface oxophilicity and regulate the electronic structure. This modification weakens *CO adsorption and increases the affinity for hydroxyl species, as supported by *in situ* experiments and DFT calculations. This synergistic effect prevents over-oxidation and boosts GA synthesis, achieving a FE of 93.8% and stable cyclic electrolysis over 100 h [109].

4.2 Photo-electrocatalytic ethylene glycol oxidation reaction

Besides, photo-electrocatalytic upcycling of plastic waste supplies a green way for mitigating plastic pollution and enabling the synthesis of renewable fuel and valued chemicals. The electrocatalytic ethylene glycol oxidation reaction has been elaborated in detail above. Before the photo-electrocatalytic upcycling is described, we give a brief introduction of photo-reforming (PR) of plastic waste. Reisner et al. [110] proposed a sustainable pathway for plastic upcycling, known as PR of plastic waste at ambient temperature. This method utilized a suitable photo-catalyst (CdS/CdO$_x$ quantum dots) to transform PET waste into organic products. However, the drawbacks of this method lie in its low production and conversion efficiency. To address this, Qiao et al. [111] integrated defect-rich chalcogenide nanosheets ($NiPS_3$, $ReSe_2$, $NiTe_2$, and P) with photocatalysts (CdS, TiO_2, and CN_x). By integrating $NiPS_3$ nanosheets and CdS, electrons were transferred from CdS to $NiPS_3$ nanosheets. According to the theoretical calculations, photo-induced CdS holes were the main active sites for PET photo-reforming. In this regard, a sufficient quantity of CdS holes, generated by electron redistribution, contributed to high efficiency (organic yield of up to 78 μmol within 9 h) and excellent stability (over 100 h) in PET photoreforming. Zhong et al. [112] introduced iodine into polymeric carbon nitride (PCN) by adding potassium iodide (KI). The introduced iodine could help break the π–π bond and function as an inhibitor to prevent the reverse recombination of PCN. Meanwhile, K^+ was able to increase the interlayered electron transfer and thus improve charge separation ability by forming a covalent bond with N in PCN. Consequently, the synthesized hydrophilic and fragmented PCN photocatalyst showed remarkable photocatalytic activity in alkaline PET solution.

Furthermore, researchers proposed the photo-electrochemical EG oxidation route based on advancements in electro-reforming and photo-reforming of PET waste. For instance, nickel-phosphorus nanospheres (nanoNi-P) coupled with TiO_2 nanorods could act as a photoanode for photo-electrochemical EG oxidation [113]. After a CV activation process, it was characterized that the nanoNi-P was converted into a nickel oxyhydroxide ultrathin layer on top of the nanoNi-P. The nickel oxyhydroxide layer consisted of both β-NiOOH and γ-NiOOH, with β-NiOOH acting as the primary active sites for the photo-electrocatalysis of PET hydrolysate. Thanks to the presence of P species in nanoNi-P(CV), the further evolution of β-NiOOH to γ-NiOOH could be suppressed. This is beneficial for efficient PET transformation into formate, giving high selectivity and a FE of approximately 100% for formate generation.

In addition, the photo-electrochemical upcycling of PET waste can be combined with other suitable cathodic reduction reactions, such as CO_2RR for CO_2 reduction and ORR for H_2O_2 production (Fig. 9). An energy-conserving co-photoelectrolysis system was successfully implemented through the synergistic coupling of the ORR with the EGOR, using a Z-type Mo_2N-Co_3O_4@Fe_2O_3 photocathode and a Co_3O_4 photoanode. The assembled electrolyzer operated at a low voltage of 1.2 V vs. normal hydrogen electrode (NHE), effectively driving the two half reactions. The accelerated reaction kinetics facilitated by the EGOR-assisted ORR, with ORR synergistic reaction, resulted in a H_2O_2 yield that is at least three times higher than that of ORR synergistic OER [114]. Furthermore, a photoelectrochemical platform featuring a perovskite-based photocathode that integrates CO_2-reduction catalysts has been developed. The $Cu_{27}Pd_{73}$ alloy anode selectively reforms PET plastics into glycolate in an alkaline solution. This work suggests the

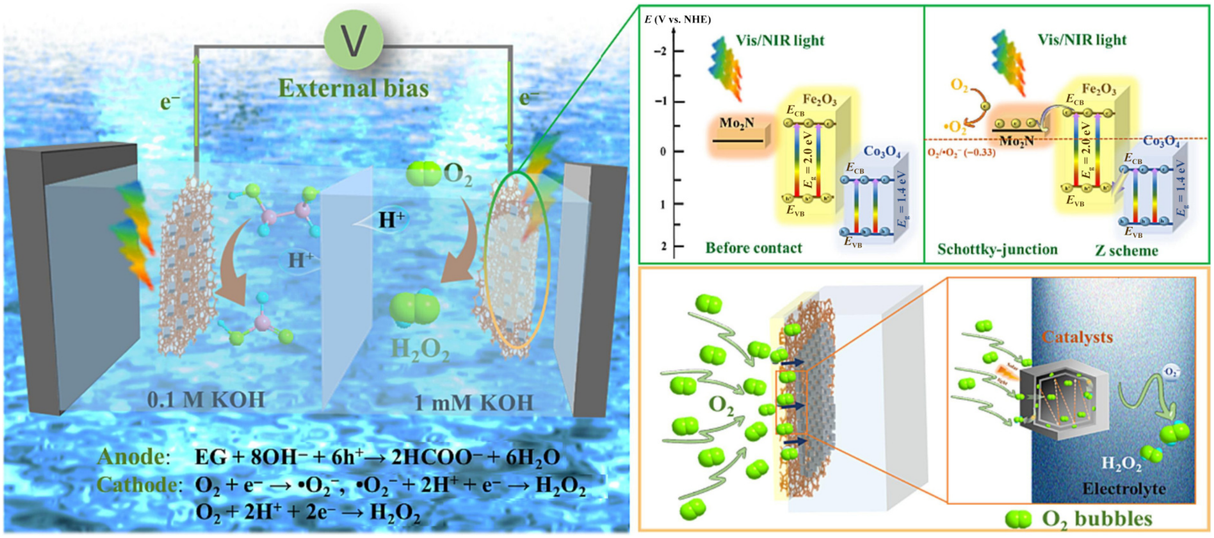

Figure 9 Proposed reaction mechanism for PEC H_2O_2 generation, and illustration of the design of cell with spontaneous H_2O_2 and formic acid generation. Reproduced with permission Ref. [114], © Elsevier B.V. 2024.

potential of photoelectrochemical CO_2-to-fuel production coupled with plastic-to-chemical conversion as a promising and sustainable technology driven by sunlight [115].

4.3 Electrocatalytic upcycling of terephthalic acid

As mentioned at the beginning of this chapter, alkaline hydrolysis can depolymerize PET into TPA and EG monomers by digestion in alkaline solutions (KOH/NaOH). The electrocatalytic upcycling of ethylene glycol monomers has been overviewed in section 4.1. In terms of the TPA upgrading, TPA can be easily precipitated and regenerated by adding acidifier to the PET electrolyte followed by filtration. In particular, terephthalic acid synthesized from the depolymerization of waste PET, is also known as BDC. And BDC as an organic linker, can be utilized to synthesize BDC-based MOFs, by reacting with a metal source. Metal organic frameworks, comprised of metal clusters bridged by organic ligands, possess unique characteristics including a porous crystalline structure and ultrahigh surface area, making them suitable for a wide range of applications, particularly in the field of energy conversion and storage [116]. With the effective use of waste PET as a BDC linker source, UiO-66(Zr) [68, 69], MIL-53(Cr, Al, Ga) [117] materials, and so on have been successfully prepared [118] through a simple hydrothermal, solvothermal, or microwave-assisted method. Considering the poor conductivity of MOFs, Park et al. [70] synthesized the CNTs-supported nanometer Ni-MOFs by reacting BDC depolymerized from PET waste with nickel source-decorated CNTs. The uniformly distributed Ni-MOFs in the highly-conductive CNT support possessed a mesoporous structure. As expected, the obtained Ni-MOF@CNT electrodes showed enhanced catalytic performance in urea oxidation reaction, exhibiting a low onset potential, fast kinetics, and great conductivity. Furthermore, this novel synthesis technique has general applicability, as evidenced by the successful synthesis of nanometer Fe-MOF/CNT nanocomposites [70].

5 Conclusion and perspective

In conclusion, poly(ethylene terephthalate) is one of the most widely used synthetic polyesters, known for its excellent durability and corrosion resistance. These properties are advantageous for applications such as single-use packaging and clothing. However, they pose substantial challenges for waste management due to the slow degradation rate of PET, which leads to significant environmental accumulation and plastic pollution, severely impacting ecosystems. In light of this, there is an urgent need to develop recycling and upcycling strategies for PET waste treatment. Great efforts have been made to establish cascade degradation and electrocatalytic upcycling strategy, serving as a “waste-to-wealth” pathway to convert PET waste into valued products.

In this review, we provide a comprehensive overview by summarizing the latest progress of “degradation-electrocatalytic upcycling” for PET waste treatment. The electrocatalytic upcycling process leverages the electrocatalytic properties of products derived from PET pyrolysis, or electro-reform its hydrolyzed intermediates, to generate high-value products. Accordingly, this review categorizes this strategy into “pyrolysis-electrocatalytic upcycling” and “hydrolysis-electrocatalytic upcycling”, followed by systematically summarizing the recent progress for each category. This approach has been shown to unlock the intrinsic value of degradation products, creating greater economic and ecological benefits compared to traditional treatment methods. Despite these advances, several challenges persist and require attention in future research (Fig. 10).

Firstly, in the PET waste degradation process, particularly during pyrolysis, controlling energy consumption and enhancing efficiency are critical. Many solutions are being explored, such as optimizing reaction conditions, employing catalysts, and investigating new technologies to improve the energy efficiency of PET pyrolysis. Further, more controlled and efficient processes are crucial for the synthesis of high-quality multi-dimensional carbon materials. Understanding the transformation mechanism from plastic to carbon under varying conditions is essential for optimizing the quality of carbon-based electrocatalysts.

Moreover, in the context of electrocatalytic upcycling, further rational regulation of catalysts from the perspective of compositions and structures is necessary to enhance catalytic efficiency. Also, developing novel catalysts with high efficiency and long-term durability holds significance. Leveraging advanced characterization techniques and computational modeling can provide insights into the synthesis process and guide the rational design of high-

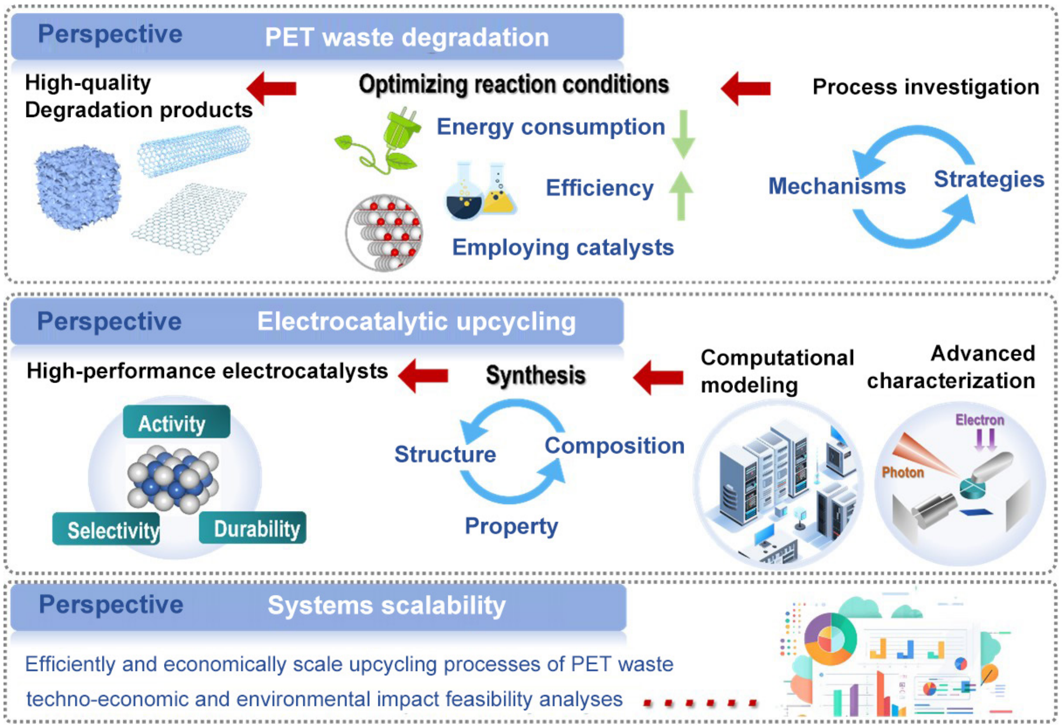

Figure 10 Schematic to illustrate the perspective of "degradation- electrocatalytic upcycling" strategy for the transformation of waste PET into valued products.

performance electrocatalysts. This approach allows for a more precise understanding of the structure–property relationships, aiding in the development of targeted synthesis strategies.

Finally, scalability of the systems remains a key goal for industrial applications. Research should focus on advancing technologies that can efficiently and economically scale upcycling processes of PET waste. To achieve this, real-world challenges need to be addressed, for example, the need to develop a cheap large-scale process to remove PET waste impurities and the separation of small molecule products for the waste upcycling. In addition, it is essential to conduct techno-economic and environmental impact feasibility analyses for the practical implementation of PET upcycling technologies. In this analysis, one should consider the energy inputs and outputs, net cost, environmental impacts so as to assess the potential value of this technology.

Looking forward, the cascade degradation and electrocatalytic upcycling of waste PET hold promise for mitigating issues related to plastic pollution and carbon emissions. It is hoped that this comprehensive review will provide valuable insights for the plastic waste treatment and inspire further advancements in the valorization of plastic waste.

Data availability

All data needed to support the conclusions in the paper are presented in the manuscript. Additional data related to this paper may be requested from the corresponding author upon request.

Acknowledgements

The authors gratefully acknowledge the support of the National key research and development program (No. 2023YFB250400), the National Natural Science Foundation of China (No. 52271222), the Science and Technology Commission of Shanghai Municipal (Nos. 23DZ1202500 and 21010503100), the Shanghai Young Outstanding Academic Leaders Plan (Overseas), and the Shanghai Pujiang Program (No. 23PJ1409300).

Declaration of competing interest

All the contributing authors report no conflict of interests in this work.

Author contribution statement

X. L.: Data curation, drawing schematics, writing manuscript, and funding acquisition. Z. J.: Data curation, drawing schematics, and writing manuscript. Z. K. and J. W.: Conceptualization and revising manuscript. S. Z.: Project administration and funding acquisition. All the authors have approved the final manuscript.

Use of AI statement

During the preparation of this work, the authors used ChatGPT in order to polish the English language quality. After using this tool/service, the authors reviewed and edited the content as needed and take full responsibility for the content of the publication.

References

[1] Borrelle, S. B.; Ringma, J.; Law, K. L.; Monnahan, C. C.; Lebreton, L.; Mcgivern, A.; Murphy, E.; Jambeck, J.; Leonard, G. H.; Hilleary, M. A. et al. Predicted growth in plastic waste exceeds efforts to mitigate plastic pollution. *Science* **2020**, *369*, 1515–1518.

[2] Martín, A. J.; Mondelli, C.; Jaydev, S. D.; Pérez-Ramírez, J. Catalytic processing of plastic waste on the rise. *Chem* **2021**, *7*, 1487–1533.

[3] Vidal, F.; van der Marel, E. R.; Kerr, R. W. F.; Mcelroy, C.; Schroeder, N.; Mitchell, C.; Rosetto, G.; Chen, T. T. D.; Bailey, R. M.; Hepburn, C. et al. Designing a circular carbon and plastics economy for a sustainable future. *Nature* **2024**, *626*, 45–57.

[4] Taniguchi, I.; Yoshida, S.; Hiraga, K.; Miyamoto, K.; Kimura, Y.; Oda, K. Biodegradation of PET: Current status and application aspects. *ACS Catal.* **2019**, *9*, 4089–4105.

[5] Lange, J. P. Managing plastic waste-sorting, recycling, disposal, and product redesign. *ACS Sustanin. Chem. Eng.* **2021**, *9*, 15722–15738.

[6] Kang, S. L.; Sun, T.; Ma, Y. X.; Du, M. M.; Gong, M. F.; Zhou, C. Y.; Chai, Y.; Qiu, B. C. Artificial photosynthesis bringing new vigor into plastic wastes. *SmartMat* **2023**, *4*, e1202.

[7] Ashraf, M.; Ullah, N.; Khan, I.; Tremel, W.; Ahmad, S.; Tahir, M. N. Photoreforming of waste polymers for sustainable hydrogen fuel and chemicals feedstock: Waste to energy. *Chem. Rev.* **2023**, *123*, 4443–4509.

[8] Diao, J. J.; Hu, Y. F.; Tian, Y. X.; Carr, R.; Moon, T. S. Upcycling of poly(ethylene terephthalate) to produce high-value bio-products. *Cell Rep.* **2023**, *42*, 111908.

[9] Behera, S.; Dinda, S.; Saha, R.; Mondal, B. Quantitative electrocatalytic upcycling of polyethylene terephthalate plastic and its oligomer with a cobalt-based one-dimensional coordination polymer having open metal sites along with coproduction of hydrogen. *ACS Catal.* **2023**, *13*, 469–474.

[10] Singh, A. K.; Bedi, R.; Kaith, B. S. Composite materials based on recycled polyethylene terephthalate and their properties-A comprehensive review. *Compos. Part B: Eng.* **2021**, *219*, 108928.

[11] Cho, J.; Kim, B.; Kwon, T.; Lee, K.; Choi, S. I. Electrocatalytic upcycling of plastic waste. *Green Chem.* **2023**, *25*, 8444–8458.

[12] Su, H. C.; Hu, Y. J.; Feng, H. Y.; Zhu, L. J.; Wang, S. R. Efficient H_2 production from PET plastic wastes over mesoporous carbon-supported Ru-ZnO catalysts in a mild pure-water system. *ACS Sustain. Chem. Eng.* **2023**, *11*, 578–586.

[13] Zhao, X. H.; Korey, M.; Li, K.; Copenhaver, K.; Tekinalp, H.; Celik, S.; Kalaitzidou, K.; Ruan, R.; Ragauskas, A. J.; Ozcan, S. Plastic waste upcycling toward a circular economy. *Chem. Eng. J.* **2022**, *428*, 131928.

[14] Jiao, X. C.; Zheng, K.; Hu, Z. X.; Zhu, S.; Sun, Y. F.; Xie, Y. Conversion of waste plastics into value-added carbonaceous fuels under mild conditions. *Adv. Mater.* **2021**, *33*, 2005192.

[15] Su, J.; Li, T.; Xie, W.; Wang, C.; Yin, L. J.; Yan, T. R.; Wang, K. G. Emerging technologies for waste plastic treatment. *ACS Sustain. Chem. Eng.* **2023**, *11*, 8176–8192.

[16] Du, M. M.; Xing, M. Y.; Kang, S. L.; Ma, Y. X.; Qiu, B. C.; Chai, Y. Building a bridge from solid wastes to solar fuels and chemicals via artificial photosynthesis. *EcoMat* **2022**, *4*, e12259.

[17] Vollmer, I.; Jenks, M. J. F.; Roelands, M. C. P.; White, R. J.; van Harmelen, T.; de Wild, P.; van der Laan, G. P.; Meirer, F.; Keurentjes, J. T. F.; Weckhuysen, B. M. Beyond mechanical recycling: Giving new life to plastic waste. *Angew. Chem., Int. Ed.* **2020**, *59*, 15402–15423.

[18] Liu, K. S.; Wang, Y. X.; Liu, F. L.; Liu, C. X.; Shi, R.; Chen, Y. Selective electrocatalytic reforming of PET-derived ethylene glycol to formate with a Faraday efficiency of 93.2% at industrial-level current densities. *Chem. Eng. J.* **2023**, *473*, 145292.

[19] Yan, Y. F.; Zhou, H.; Xu, S. M.; Yang, J. R.; Hao, P. J.; Cai, X.; Ren, Y.; Xu, M.; Kong, X. G.; Shao, M. F. et al. Electrocatalytic upcycling of biomass and plastic wastes to biodegradable polymer monomers and hydrogen fuel at high current densities. *J. Am. Chem. Soc.* **2023**, *145*, 6144–6155.

[20] Karimi Estahbanati, M. R.; Kong, X. Y.; Eslami, A.; Soo, H. S. Current developments in the chemical upcycling of waste plastics using alternative energy sources. *ChemSusChem* **2021**, *14*, 4152–4166.

[21] Singh, A.; Rorrer, N. A.; Nicholson, S. R.; Erickson, E.; Desveaux, J. S.; Avelino, A. F. T.; Lamers, P.; Bhatt, A.; Zhang, Y. M.; Avery, G. et al. Techno-economic, life-cycle, and socioeconomic impact analysis of enzymatic recycling of poly(ethylene terephthalate). *Joule* **2021**, *5*, 2479–2503.

[22] Li, X.; Wang, J. Y.; Zhang, T.; Yang, S.; Sun, M. Z.; Qian, X. F.; Wang, T. F.; Zhao, Y. X. Sustainable catalytic strategies for the transformation of plastic wastes into valued products. *Chem. Eng. Sci.* **2023**, *276*, 118729.

[23] Zheng, K.; Wu, Y.; Hu, Z. X.; Wang, S. M.; Jiao, X. C.; Zhu, J. C.; Sun, Y. F.; Xie, Y. Progress and perspective for conversion of plastic wastes into valuable chemicals. *Chem. Soc. Rev.* **2023**, *52*, 8–29.

[24] Hou, P. X.; Zhang, F.; Zhang, L. L.; Liu, C.; Cheng, H. M. Synthesis of carbon nanotubes by floating catalyst chemical vapor deposition and their applications. *Adv. Funct. Mater.* **2022**, *32*, 2108541.

[25] Tang, L.; Tan, J. Y.; Nong, H. Y.; Liu, B. L.; Cheng, H. M. Chemical vapor deposition growth of two-dimensional compound materials: Controllability, material quality, and growth mechanism. *Acc. Mater. Res.* **2021**, *2*, 36–47.

[26] Zhang, J.; Wang, F.; Shenoy, V. B.; Tang, M.; Lou, J. Towards controlled synthesis of 2D crystals by chemical vapor deposition (CVD). *Mater. Today* **2020**, *40*, 132–139.

[27] Veksha, A.; Yin, K.; Moo, J. G. S.; Oh, W. D.; Ahamed, A.; Chen, W. Q.; Weerachanchai, P.; Giannis, A.; Lisak, G. Processing of flexible plastic packaging waste into pyrolysis oil and multi-walled carbon nanotubes for electrocatalytic oxygen reduction. *J. Hazardous Mater.* **2020**, *387*, 121256.

[28] Chen, W. Q.; Fu, X. X.; Chan, W. P.; Veksha, A.; Lisak, G. Carbon nanosheet-carbon nanocage encapsulated Cu composite from chemical vapor deposition of real-world plastic waste for tailored CO_2 conversion to various products. *Appl. Mater. Today* **2021**, *25*, 101207.

[29] Sangeetha, D. N.; Santosh, M. S.; Selvakumar, M. Flower-like carbon doped MoS_2/activated carbon composite electrode for superior performance of supercapacitors and hydrogen evolution reactions. *J. Alloys Compd.* **2020**, *831*, 154745.

[30] Veeramani, K.; Janani, G.; Kim, J.; Surendran, S.; Lim, J.; Jesudass, S. C.; Mahadik, S.; Lee, H.; Kim, T. H.; Kim, J. K. et al. Hydrogen and value-added products yield from hybrid water electrolysis: A critical review on recent developments. *Renew. Sustain. Energy Rev.* **2023**, *177*, 113227.

[31] Wang, Y.; Liu, J. L.; Yuan, H. J.; Liu, F.; Hu, T. J.; Yang, B. Q. Strong electronic interaction between amorphous MnO_2 nanosheets and ultrafine Pd nanoparticles toward enhanced oxygen reduction and ethylene glycol oxidation reactions. *Adv. Funct. Mater.* **2023**, *33*, 2211909.

[32] Li, J. S.; Li, L. M.; Ma, X. Y.; Han, X.; Xing, C. C.; Qi, X. Q.; He, R.; Arbiol, J.; Pan, H. Y.; Zhao, J. et al. Selective ethylene glycol oxidation to formate on nickel selenide with simultaneous evolution of hydrogen. *Adv. Sci.* **2023**, *10*, 2300841.

[33] Yan, H.; Yao, S.; Wang, J. Y.; Zhao, S. M.; Sun, Y. H.; Liu, M. Y.; Zhou, X.; Zhang, G. Y.; Jin, X.; Feng, X. et al. Engineering Pt-Mn_2O_3 interface to boost selective oxidation of ethylene glycol to glycolic acid. *Appl. Catal. B: Environ.* **2021**, *284*, 119803.

[34] Wang, J. Y.; Li, X.; Zhang, T.; Qian, X. F.; Wang, T. F.; Zhao, Y. X. Rational design of photo-/electro-catalytic systems for the transformation of plastic wastes. *Appl. Catal. B: Environ.* **2023**, *332*, 122744.

[35] Wang, H. J.; Zhan, W. J.; Yu, H. J.; Jiang, S. J.; Wang, B. B.; Deng, K.; Wang, Z. Q.; Xu, Y.; Wang, L. Nitrogen-doped Ni_3P-$NiMoO_4$ heterostructure arrays for coupling hydrogen production with polyethylene terephthalate plastic electro-recycling. *Mater. Today Phys.* **2023**, *37*, 101192.

[36] Moges, E. A.; Chang, C. Y.; Tsai, M. C.; Su, W. N.; Hwang, B. J. Electrocatalysts for value-added electrolysis coupled with hydrogen evolution. *EES Catal.* **2023**, *1*, 413–433.

[37] Du, J. L.; Xiang, D. L.; Zhou, K. X.; Wang, L. C.; Yu, J. Y.; Xia, H. H.; Zhao, L. L.; Liu, H.; Zhou, W. J. Electrochemical hydrogen production coupled with oxygen evolution, organic synthesis, and waste reforming. *Nano Energy* **2022**, *104*, 107875.

[38] Zhou, H.; Wang, Y.; Ren, Y.; Li, Z. H.; Kong, X. G.; Shao, M. F.;

Duan, H. H. Plastic waste valorization by leveraging multidisciplinary catalytic technologies. *ACS Catal.* **2022**, *12*, 9307–9324.

[39] Roy, P. S.; Garnier, G.; Allais, F.; Saito, K. Strategic approach towards plastic waste valorization: Challenges and promising chemical upcycling possibilities. *ChemSusChem* **2021**, *14*, 4007–4027.

[40] Chen, X.; Wang, Y. D.; Zhang, L. Recent progress in the chemical upcycling of plastic wastes. *ChemSusChem* **2021**, *14*, 4137–4151.

[41] Ge, R. X.; Li, J.; Duan, H. H. Recent advances in non-noble electrocatalysts for oxidative valorization of biomass derivatives. *Sci. China Mater.* **2022**, *65*, 3273–3301.

[42] Li, Y. H.; Ozden, A.; Leow, W. R.; Ou, P. F.; Huang, J. E.; Wang, Y. H.; Bertens, K.; Xu, Y.; Liu, Y.; Roy, C. et al. Redox-mediated electrosynthesis of ethylene oxide from CO_2 and water. *Nat. Catal.* **2022**, *5*, 185–192.

[43] Papanikolaou, G.; Centi, G.; Perathoner, S.; Lanzafame, P. Catalysis for e-chemistry: Need and gaps for a future De-fossilized chemical production, with focus on the role of complex (direct) syntheses by electrocatalysis. *ACS Catal.* **2022**, *12*, 2861–2876.

[44] Kim, S.; Kong, D.; Zheng, X. L.; Park, J. H. Upcycling plastic wastes into value-added products via electrocatalysis and photoelectrocatalysis. *J. Energy Chem.* **2024**, *91*, 522–541.

[45] Lou, X. X.; Liu, F. Y.; Li, Q. Y.; Chu, M. Y.; Wang, G. L.; Chen, J. X.; Cao, M. H. Advances in solar-driven, electro/photoelectrochemical, and microwave-assisted upcycling of waste polyesters. *Chem. Commun.* **2024**, *60*, 2828–2838.

[46] Li, J. N.; Ma, H. P.; Zhao, G. P.; Huang, G. F.; Sun, W. B.; Peng, C. Plastic waste conversion by leveraging renewable photo/electro-catalytic technologies. *ChemSusChem* **2024**, *17*, e202301352.

[47] Sajwan, D.; Sharma, A.; Sharma, M.; Krishnan, V. Upcycling of plastic waste using photo-, electro-, and photoelectrocatalytic approaches: A way toward circular economy. *ACS Catal.* **2024**, *14*, 4865–4926.

[48] Barnard, E.; Rubio Arias, J. J.; Thielemans, W. Chemolytic depolymerisation of PET: A review. *Green Chem.* **2021**, *23*, 3765–3789.

[49] Lu, H. Y.; Diaz, D. J.; Czarnecki, N. J.; Zhu, C. Z.; Kim, W.; Shroff, R.; Acosta, D. J.; Alexander, B. R.; Cole, H. O.; Zhang, Y. et al. Machine learning-aided engineering of hydrolases for PET depolymerization. *Nature* **2022**, *604*, 662–667.

[50] Dhaka, V.; Singh, S.; Anil, A. G.; Sunil Kumar Naik, T. S.; Garg, S.; Samuel, J.; Kumar, M.; Ramamurthy, P. C.; Singh, J. Occurrence, toxicity and remediation of polyethylene terephthalate plastics. A review. *Environ. Chem. Lett.* **2022**, *20*, 1777–1800.

[51] Wei, R.; Breite, D.; Song, C.; Gräsing, D.; Ploss, T.; Hille, P.; Schwerdtfeger, R.; Matysik, J.; Schulze, A.; Zimmermann, W. Biocatalytic degradation efficiency of postconsumer polyethylene terephthalate packaging determined by their polymer microstructures. *Adv. Sci.* **2019**, *6*, 1900491.

[52] Huang, J. B.; Meng, H. X.; Luo, X. S.; Mu, X.; Xu, W. W.; Jin, L.; Lai, B. S. Insights into the thermal degradation mechanisms of polyethylene terephthalate dimer using DFT method. *Chemosphere* **2022**, *291*, 133112.

[53] Zhou, N.; Dai, L. L.; Lv, Y. C.; Li, H.; Deng, W. Y.; Guo, F. Q.; Chen, P.; Lei, H. W.; Ruan, R. Catalytic pyrolysis of plastic wastes in a continuous microwave assisted pyrolysis system for fuel production. *Chem. Eng. J.* **2021**, *418*, 129412.

[54] Çepelioğullar, Ö.; Pütün, A. E. A pyrolysis study for the thermal and kinetic characteristics of an agricultural waste with two different plastic wastes. *Waste Manag. Res.* **2014**, *32*, 971–979.

[55] Jiang, M. K.; Wang, X. L.; Xi, W. L.; Zhou, H. X.; Yang, P.; Yao, J. L.; Jiang, X. L.; Wu, D. Upcycling plastic waste to carbon materials for electrochemical energy storage and conversion. *Chem. Eng. J.* **2023**, *461*, 141962.

[56] Choi, J.; Yang, I.; Kim, S. S.; Cho, S. Y.; Lee, S. Upcycling plastic waste into high value-added carbonaceous materials. *Macromol. Rapid Commun.* **2022**, *43*, 2100467.

[57] Fitzer, E.; Kochling, K. H.; Boehm, H. P.; Marsh, H. Recommended terminology for the description of carbon as a solid (IUPAC Recommendations 1995). *Pure Appl. Chem.* **1995**, *67*, 473–506.

[58] Dai, L. L.; Karakas, O.; Cheng, Y. L.; Cobb, K.; Chen, P.; Ruan, R. A review on carbon materials production from plastic wastes. *Chem. Eng. J.* **2023**, *453*, 139725.

[59] Zhao, X.; Boruah, B.; Chin, K. F.; Đokić, M.; Modak, J. M.; Soo, H. S. Upcycling to sustainably reuse plastics. *Adv. Mater.* **2022**, *34*, 2100843.

[60] Wang, C. L.; Han, H. G.; Wu, Y. F.; Astruc, D. Nanocatalyzed upcycling of the plastic wastes for a circular economy. *Coord. Chem. Rev.* **2022**, *458*, 214422.

[61] Yue, S.; Wang, P. F.; Yu, B. N.; Zhang, T.; Zhao, Z. Y.; Li, Y.; Zhan, S. H. From plastic waste to treasure: Selective upcycling through catalytic technologies. *Adv. Energy Mater.* **2023**, *13*, 2302008.

[62] Kong, D. B.; Lv, W.; Liu, R. L.; He, Y. B.; Wu, D. C.; Li, F.; Fu, R. W.; Yang, Q. H.; Kang, F. Y. Superstructured carbon materials: Design and energy applications. *Energy Mater. Devices* **2023**, *1*, 9370017.

[63] Li, Y.; Wang, H. H.; Priest, C.; Li, S. W.; Xu, P.; Wu, G. Electrocatalysis: Advanced electrocatalysis for energy and environmental sustainability via water and nitrogen reactions. *Adv. Mater.* **2021**, *33*, 2170042.

[64] Yan, C. C.; Jiang, X.; Yu, J. X.; Ding, Z. L.; Ma, L.; Su, T. Y.; Wang, Y. L.; Wang, C. X.; Huang, G. Y.; Xu, S. M. Waste to wealth: Direct utilization of spent materials for electrocatalysis and energy storage. *Green Chem.* **2023**, *25*, 3816–3846.

[65] Chen, C. C.; Han, X.; Li, X.; Jiang, P. C.; Niu, D.; Ma, L. X.; Liu, W. D.; Li, S. Y.; Qu, Y. Y.; Hu, H. B. et al. General features to enhance enzymatic activity of poly(ethylene terephthalate) hydrolysis. *Nat. Catal.* **2021**, *4*, 425–430.

[66] Stanica-Ezeanu, D.; Matei, D. Natural depolymerization of waste poly(ethylene terephthalate) by neutral hydrolysis in marine water. *Sci. Rep.* **2021**, *11*, 4431.

[67] Saeed, B.; Khan, P.; Laeeq Khan, A.; Almohamadi, H.; Naeem, A.; Aslam, M.; Zaman, M.; Niazi, M. B. K.; Amjad Gilani, M.; Yasin, M. Experimental and theoretical insights into bioethanol recovery: Valorizing waste PET bottles for sustainable pervaporation membranes. *Sep. Purif. Technol.* **2025**, *357*, 130104.

[68] Dyosiba, X.; Ren, J. W.; Musyoka, N. M.; Langmi, H. W.; Mathe, M.; Onyango, M. S. Feasibility of varied polyethylene terephthalate wastes as a linker source in metal-organic framework UiO-66(Zr) synthesis. *Ind. Eng. Chem. Res.* **2019**, *58*, 17010–17016.

[69] Singh, S.; Sharma, S.; Umar, A.; Jha, M.; Mehta, S. K.; Kansal, S. K. Nanocuboidal-shaped zirconium based metal organic framework for the enhanced adsorptive removal of nonsteroidal anti-inflammatory drug, ketorolac tromethamine, from aqueous phase. *New J. Chem.* **2018**, *42*, 1921–1930.

[70] Gangaraju, D.; Shanmugharaj, A. M.; Sridhar, V.; Park, H. Fabrication of nanometer-sized nickel-based metal organic frameworks on carbon nanotubes for electro-catalytic oxidation of urea and arsenic removal. *ACS Appl. Nano Mater.* **2022**, *5*, 19035–19042.

[71] Mellmann, D.; Sponholz, P.; Junge, H.; Beller, M. Formic acid as a hydrogen storage material-development of homogeneous catalysts for selective hydrogen release. *Chem. Soc. Rev.* **2016**, *45*, 3954–3988.

[72] Li, L.; Ozden, A.; Guo, S. Y.; de Arquer, F. P. G.; Wang, C. H.; Zhang, M. Z.; Zhang, J.; Jiang, H. Y.; Wang, W.; Dong, H. et al. Stable, active CO_2 reduction to formate via redox-modulated stabilization of active sites. *Nat. Commun.* **2021**, *12*, 5223.

[73] Si, D.; Xiong, B. Y.; Chen, L. S.; Shi, J. L. Highly selective and

efficient electrocatalytic synthesis of glycolic acid in coupling with hydrogen evolution. Chem. Catal. **2021**, *1*, 941–955.

[74] Qi, J.; An, Z. Y.; Li, C.; Chen, X.; Li, W. Z.; Liang, C. H. Electrocatalytic selective oxidation of ethylene glycol: A concise review of catalyst development and reaction mechanism with comparison to thermocatalytic oxidation process. Curr. Opin. Electroche. **2022**, *32*, 100929.

[75] Chauhan, N. L.; Dameera, V.; Chowdhury, A.; Juvekar, V. A.; Sarkar, A. Electrochemical oxidation of ethylene glycol in a channel flow reactor. Catal. Today **2018**, *309*, 126–132.

[76] Juan, C.; Lan, B.; Zhao, C. C.; Zhang, H. L.; Li, D.; Zhang, F. From waste plastics to layered porous nitrogen-doped carbon materials with excellent HER performance. Chem. Commun. **2023**, *59*, 6187–6190.

[77] Muhyuddin, M.; Mustarelli, P.; Santoro, C. Recent advances in waste plastic transformation into valuable platinum-group metal-free electrocatalysts for oxygen reduction reaction. ChemSusChem **2021**, *14*, 3785–3800.

[78] Liu, X. G.; Ma, C. D.; Wen, Y. L.; Chen, X. C.; Zhao, X.; Tang, T.; Holze, R.; Mijowska, E. Highly efficient conversion of waste plastic into thin carbon nanosheets for superior capacitive energy storage. Carbon **2021**, *171*, 819–828.

[79] Min, J. K.; Wen, X.; Tang, T.; Chen, X. C.; Huo, K. F.; Gong, J.; Azadmanjiri, J.; He, C. B.; Mijowska, E. A general approach towards carbonization of plastic waste into a well-designed 3D porous carbon framework for super lithium-ion batteries. Chem. Commun. **2020**, *56*, 9142–9145.

[80] Li, C. P.; Tong, L. J.; Wang, S. L.; Liu, Q.; Wang, Y. X.; Li, X.; Wang, M. X.; Li, M. X.; Chen, X. C.; Wu, J. X. et al. Nitrogen doping induced by intrinsic defects of recycled polyethylene terephthalate-derived carbon nanotubes. SusMat **2023**, *3*, 431–440.

[81] Moo, J. G. S.; Veksha, A.; Oh, W. D.; Giannis, A.; Udayanga, W. D. C.; Lin, S. X.; Ge, L. Y.; Lisak, G. Plastic derived carbon nanotubes for electrocatalytic oxygen reduction reaction: Effects of plastic feedstock and synthesis temperature. Electrochem. Commun. **2019**, *101*, 11–18.

[82] Zhang, Y.; Zhang, L. Y.; Zhou, C. W. Review of chemical vapor deposition of graphene and related applications. Acc. Chem. Res. **2013**, *46*, 2329–2339.

[83] Wang, Q. C.; Lei, Y. P.; Wang, Y. C.; Liu, Y.; Song, C. Y.; Zeng, J.; Song, Y. H.; Duan, X. D.; Wang, D. S.; Li, Y. D. Atomic-scale engineering of chemical-vapor-deposition-grown 2D transition metal dichalcogenides for electrocatalysis. Energy Environ. Sci. **2020**, *13*, 1593–1616.

[84] Luong, D. X.; Bets, K. V.; Algozeeb, W. A.; Stanford, M. G.; Kittrell, C.; Chen, W. Y.; Salvatierra, R. V.; Ren, M. Q.; Mchugh, E. A.; Advincula, P. A. et al. Gram-scale bottom-up flash graphene synthesis. Nature **2020**, *577*, 647–651.

[85] Algozeeb, W. A.; Savas, P. E.; Luong, D. X.; Chen, W. Y.; Kittrell, C.; Bhat, M.; Shahsavari, R.; Tour, J. M. Flash graphene from plastic waste. ACS Nano **2020**, *14*, 15595–15604.

[86] Chia, X.; Pumera, M. Characteristics and performance of two-dimensional materials for electrocatalysis. Nat. Catal. **2018**, *1*, 909–921.

[87] Wu, X. Z.; Xiao, S. T.; Long, Y. P.; Ma, T.; Shao, W. J.; Cao, S. J.; Xiang, X.; Ma, L.; Qiu, L.; Cheng, C. et al. Emerging 2D materials for electrocatalytic applications: Synthesis, multifaceted nanostructures, and catalytic center design. Small **2022**, *18*, 2105831.

[88] Jorge, A. B.; Jervis, R.; Periasamy, A. P.; Qiao, M.; Feng, J. Y.; Tran, L. N.; Titirici, M. M. 3D carbon materials for efficient oxygen and hydrogen electrocatalysis. Adv. Energy Mater. **2020**, *10*, 1902494.

[89] Zhou, H.; Ren, Y.; Li, Z. H.; Xu, M.; Wang, Y.; Ge, R. X.; Kong, X. G.; Zheng, L. R.; Duan, H. H. Electrocatalytic upcycling of polyethylene terephthalate to commodity chemicals and H_2 fuel. Nat. Commun. **2021**, *12*, 4679.

[90] Wang, N.; Li, X. F.; Hu, M. K.; Wei, W. B.; Zhou, S. H.; Wu, X. T.; Zhu, Q. L. Ordered macroporous superstructure of bifunctional cobalt phosphide with heteroatomic modification for paired hydrogen production and polyethylene terephthalate plastic recycling. Appl. Catal. B: Environ. **2022**, *316*, 121667.

[91] Li, Z. J.; Yang, Z. H.; Wang, S.; Luo, H. X.; Xue, Z. M.; Liu, Z. H.; Mu, T. C. Medium entropy metal oxide induced *OH species targeted transfer strategy for efficient polyethylene terephthalate plastic recycling. Chem. Eng. J. **2024**, *479*, 147611.

[92] Li, Y.; Lee, L. Q.; Yu, Z. G.; Zhao, H.; Zhang, Y. W.; Gao, P. Q.; Li, H. Coupling of PET waste electroreforming with green hydrogen generation using bifunctional catalyst. Sustain. Energy Fuels **2022**, *6*, 4916–4924.

[93] Chang, J. L.; Wang, L. L.; Wu, D. P.; Xu, F.; Jiang, K.; Guo, Y. M.; Gao, Z. Y. Concurrent electrocatalytic hydrogen evolution and polyethylene terephthalate plastics reforming by self-supported amorphous cobalt iron phosphide electrode. J. Colloid Interface Sci. **2024**, *655*, 555–564.

[94] Zhang, X. Y.; Wei, R. R.; Yan, M.; Wang, X. L.; Wei, X. W.; Wang, Y. L.; Wang, L.; Zhang, J. M.; Yin, S. L. One-pot synthesis inorganic-organic hybrid PdNi bimetallenes for PET electrocatalytic value-added transformation. Adv. Funct. Mater. **2024**, *34*, 2401796.

[95] Aziz, A.; Yu, W.; Tang, R.; Crespo-Otero, R.; Tommaso, D. D.; Nishihara, H. Theoretical insights into the role of defects in the optimization of the electrochemical capacitance of graphene. Energy Mater. Devices **2024**, *2*, 9370035.

[96] Liu, X.; Fang, Z. Y.; Xiong, D. K.; Gong, S. Q.; Niu, Y. L.; Chen, W.; Chen, Z. F. Upcycling PET in parallel with energy-saving H_2 production via bifunctional nickel-cobalt nitride nanosheets. Nano Res. **2023**, *16*, 4625–4633.

[97] Chen, Z. J.; Wei, W.; Shen, Y. S.; Ni, B. J. Defective nickel sulfide hierarchical structures for efficient electrochemical conversion of plastic waste to value-added chemicals and hydrogen fuel. Green Chem. **2023**, *25*, 5979–5988.

[98] Mao, Y.; Fan, S. Y.; Li, X. Y.; Shi, J. G.; Wang, M. F.; Niu, Z. D.; Chen, G. H. Trash to treasure: Electrocatalytic upcycling of polyethylene terephthalate (PET) microplastic to value-added products by $Mn_{0.1}Ni_{0.9}Co_2O_{4-\delta}$ RSFs spinel. J. Hazardous Mater. **2023**, *457*, 131743.

[99] Liu, X.; Fang, Z.; Teng, X.; Niu, Y.; Gong, S.; Chen, W.; Meyer, T. J.; Chen, Z. Paired formate and H_2 productions via efficient bifunctional Ni–Mo nitride nanowire electrocatalysts. J. Energy Chem. **2022**, *72*, 432–441.

[100] Zhang, H. G.; Wang, Y. L.; Li, X. M.; Deng, K.; Yu, H. J.; Xu, Y.; Wang, H. J.; Wang, Z. Q.; Wang, L. Electrocatalytic upcycling of polyethylene terephthalate plastic to formic acid coupled with energy-saving hydrogen production over hierarchical Pd-doped NiTe nanoarrays. Appl. Catal. B: Environ. **2024**, *340*, 123236.

[101] Kang, H. X.; He, D.; Yan, X. X.; Dao, B. M.; Williams, N. B.; Elliott, G. I.; Streater, D.; Nyakuchena, J.; Huang, J. E.; Pan, X. Q. et al. Cu promoted the dynamic evolution of Ni-based catalysts for polyethylene terephthalate plastic upcycling. ACS Catal. **2024**, *14*, 5314–5325.

[102] Na, J.; Seo, B.; Kim, J.; Lee, C. W.; Lee, H.; Hwang, Y. J.; Min, B. K.; Lee, D. K.; Oh, H. S.; Lee, U. General technoeconomic analysis for electrochemical coproduction coupling carbon dioxide reduction with organic oxidation. Nat. Commun. **2019**, *10*, 5193.

[103] Wang, J. Y.; Li, X.; Wang, M. L.; Zhang, T.; Chai, X. Y.; Lu, J. L.; Wang, T. F.; Zhao, Y. X.; Ma, D. Electrocatalytic valorization of poly(ethylene terephthalate) plastic and CO_2 for simultaneous production of formic acid. ACS Catal. **2022**, *12*, 6722–6728.

[104] Qi, J.; Du, Y. D.; Yang, Q.; Jiang, N.; Li, J. C.; Ma, Y.; Ma, Y. J.;

Zhao, X.; Qiu, J. S. Energy-saving and product-oriented hydrogen peroxide electrosynthesis enabled by electrochemistry pairing and product engineering. *Nat. Commun.* **2023**, *14*, 6263.

[105] Ren, T. L.; Yu, Z.; Yu, H. J.; Deng, K.; Wang, Z. Q.; Li, X. N.; Wang, H. J.; Wang, L.; Xu, Y. Sustainable ammonia electrosynthesis from nitrate wastewater coupled to electrocatalytic upcycling of polyethylene terephthalate plastic waste. *ACS Nano* **2023**, *17*, 12422–12432.

[106] Liu, F. L.; Gao, X. T.; Shi, R.; Guo, Z. X.; Tse, E. C. M.; Chen, Y. Concerted and selective electrooxidation of polyethylene-terephthalate-derived alcohol to glycolic acid at an industry-level current density over a Pd-Ni(OH)$_2$ Catalyst. *Angew. Chem., Int. Ed.* **2023**, *62*, e202300094.

[107] Liu, X.; He, X. Y.; Xiong, D. K.; Wang, G. Y.; Tu, Z. T.; Wu, D. L.; Wang, J. Y.; Gu, J.; Chen, Z. F. Electro-reforming of PET plastic to C$_2$ chemicals with concurrent generation of hydrogen and electric energy. *ACS Catal.* **2024**, *14*, 5366–5376.

[108] Wang, Y. X.; Liu, K. S.; Liu, F. L.; Liu, C. X.; Shi, R.; Chen, Y. Selective electro-reforming of waste polyethylene terephthalate-derived ethylene glycol into C$_2$ chemicals with long-term stability. *Green Chem.* **2023**, *25*, 5872–5877.

[109] Chen, J. L.; Jiang, M. M.; Zhang, F. Z.; Wang, L.; Yang, J. P. Interstitial boron atoms in Pd aerogel selectively switch the pathway for glycolic acid synthesis from waste plastics. *Adv. Mater.* **2024**, *36*, 2401867.

[110] Uekert, T.; Kuehnel, M. F.; Wakerley, D. W.; Reisner, E. Plastic waste as a feedstock for solar-driven H$_2$ generation. *Energy Environ. Sci.* **2018**, *11*, 2853–2857.

[111] Zhang, S.; Li, H. B.; Wang, L.; Liu, J. D.; Liang, G. J.; Davey, K.; Ran, J. R.; Qiao, S. Z. Boosted photoreforming of plastic waste via defect-rich NiPS$_3$ nanosheets. *J. Am. Chem. Soc.* **2023**, *145*, 6410–6419.

[112] Liu, X.; Yang, Y.; Wan, S. P.; Li, S.; Ou, M.; Song, F. J.; Fan, X.; Zhong, Q. Tuning the surface hydrophilicity of a C$_3$N$_4$ nanosheet for efficient photocatalytic H$_2$ evolution coupled with microplastic degradation. *Int. J. Hydrogen Energy* **2023**, *48*, 27599–27610.

[113] Lin, C. Y.; Huang, S. C.; Lin, Y. G.; Hsu, L. C.; Yi, C. T. Electrosynthesized Ni-P nanospheres with high activity and selectivity towards photoelectrochemical plastics reforming. *Appl. Catal. B: Environ.* **2021**, *296*, 120351.

[114] Feng, X.; Yang, L. J.; Zhang, L. Sustainable solar-and electro-driven production of high concentration H$_2$O$_2$ coupled to electrocatalytic upcycling of polyethylene terephthalate plastic waste. *Chem. Eng. J.* **2024**, *482*, 149191.

[115] Bhattacharjee, S.; Rahaman, M.; Andrei, V.; Miller, M.; Rodríguez-Jiménez, S.; Lam, E.; Pornrungroj, C.; Reisner, E. Photoelectrochemical CO$_2$-to-fuel conversion with simultaneous plastic reforming. *Nat. Synth.* **2023**, *2*, 182–192.

[116] Wang, Q.; Astruc, D. State of the art and prospects in metal-organic framework (MOF)-based and MOF-derived nanocatalysis. *Chem. Rev.* **2020**, *120*, 1438–1511.

[117] Lo, S. H.; Senthil Raja, D.; Chen, C. W.; Kang, Y. H.; Chen, J. J.; Lin, C. H. Waste polyethylene terephthalate (PET) materials as sustainable precursors for the synthesis of nanoporous MOFs, MIL-47, MIL-53(Cr, Al, Ga) and MIL-101(Cr). *Dalton Trans.* **2016**, *45*, 9565–9573.

[118] Ren, J. W.; Dyosiba, X.; Musyoka, N. M.; Langmi, H. W.; North, B. C.; Mathe, M.; Onyango, M. S. Green synthesis of chromium-based metal-organic framework (Cr-MOF) from waste polyethylene terephthalate (PET) bottles for hydrogen storage applications. *Int. J. Hydrogen Energy* **2016**, *41*, 18141–18146.